Histone Deacetylase Inhibition Blunts Ischemia/Reperfusion Injury by Inducing Cardiomyocyte Autophagy

Min Xie, Yongli Kong, Wei Tan, Herman May, Pavan K. Battiprolu, Zully Pedrozo, Zhao V. Wang, Cyndi Morales, Xiang Luo, Geoffrey Cho, Nan Jiang, Michael E. Jessen, John J. Warner, Sergio Lavandero, Thomas G. Gillette, Aslan T. Turer and Joseph A. Hill

Circulation. 2014;129:1139-1151; originally published online January 6, 2014;
doi: 10.1161/CIRCULATIONAHA.113.002416
Circulation is published by the American Heart Association, 7272 Greenville Avenue, Dallas, TX 75231

Print ISSN: 0009-7322. Online ISSN: 1524-4539

Histone Deacetylase Inhibition Blunts Ischemia/Reperfusion Injury by Inducing Cardiomyocyte Autophagy

Min Xie, MD, PhD; Yongli Kong, MD; Wei Tan, MD; Herman May, BS; Pavan K. Battiprolu, PhD; Zully Pedrozo, PhD; Zhao V. Wang, PhD; Cyndi Morales, BS; Xiang Luo, MD, PhD; Geoffrey Cho, MD; Nan Jiang, MS; Michael E. Jessen, MD; John J. Warner, MD; Sergio Lavandero, PhD; Thomas G. Gillette, PhD; Aslan T. Turer, MD, MHS; Joseph A. Hill, MD, PhD

Background—Reperfusion accounts for a substantial fraction of the myocardial injury occurring with ischemic heart disease. Yet, no standard therapies are available targeting reperfusion injury. Here, we tested the hypothesis that suberoylanilide hydroxamic acid (SAHA), a histone deacetylase inhibitor approved for cancer treatment by the US Food and Drug Administration, will blunt reperfusion injury.

Methods and Results—Twenty-one rabbits were randomly assigned to 3 groups: (1) vehicle control, (2) SAHA pretreatment (1 day before and at surgery), and (3) SAHA treatment at the time of reperfusion only. Each arm was subjected to ischemia/reperfusion surgery (30 minutes coronary ligation, 24 hours reperfusion). In addition, cultured neonatal and adult rat ventricular cardiomyocytes were subjected to simulated ischemia/reperfusion to probe mechanism. SAHA reduced infarct size and partially rescued systolic function when administered either before surgery (pretreatment) or solely at the time of reperfusion. SAHA plasma concentrations were similar to those achieved in patients with cancer. In the infarct border zone, SAHA increased autophagic flux, assayed in both rabbit myocardium and in mice harboring an RFP-GFP-LC3 transgene. In cultured myocytes subjected to simulated ischemia/reperfusion, SAHA pretreatment reduced cell death by 40%. This reduction in cell death correlated with increased autophagic activity in SAHA-treated cells. RNAi-mediated knockdown of ATG7 and ATG5, essential autophagy proteins, abolished SAHA's cardioprotective effects.

Conclusions—The US Food and Drug Administration–approved anticancer histone deacetylase inhibitor, SAHA, reduces myocardial infarct size in a large animal model, even when delivered in the clinically relevant context of reperfusion. The cardioprotective effects of SAHA during ischemia/reperfusion occur, at least in part, through the induction of autophagic flux. **(*Circulation*. 2014;129:1139-1151.)**

Key Words: autophagy ■ cell death ■ histone deacetylases ■ myocardial infarction ■ reperfusion injury

Five million Americans have chronic heart failure, the final common pathway of many forms of heart disease and the most common discharge diagnosis in Medicare for several years running.[1] This syndrome carries a mortality of ≈50% at 5 years, and its incidence and prevalence are expanding rapidly around the globe.[2] Coronary artery disease is the leading cause of heart failure with reduced ejection fraction.[3] In the context of myocardial infarction, the extent of myocardial damage correlates directly with the extent of left ventricle (LV) remodeling.[3] Indeed, significant advances in antiplatelet and antithrombotic agents, novel devices (eg, drug-eluting stents), and an abiding focus on time to reperfusion have proven critical for decreasing infarct size and preserving systolic function.[4] Nevertheless, data from the Valsartan in Acute Myocardial Infarction Trial (VALIANT) study demonstrate that, with modern percutaneous coronary intervention, the overall mortality rate reaches 25% 3 years following ST-segment elevation myocardial infarction.[5] Thus, there appears to be a ceiling on our ability to mitigate infarct size by the restoration of coronary artery patency alone.

Editorial see p 1088
Clinical Perspective on p 1151

Ischemia is often followed by reperfusion, when the infarct-related artery recannulates, either spontaneously or in response to therapeutic intervention. This event, which restores

Received March 5, 2013; accepted November 9, 2013.

From the Departments of Internal Medicine (Cardiology) (M.X., Y.K., W.Y., H.M., P.K.B., Z.P., Z.V.W., C.M., X.L., G.C., N.J., J.J.W., S.L., T.G.G., A.T.T., J.A.H.), Cardiovascular and Thoracic Surgery (M.E.J.), Advanced Center for Chronic Diseases (ACCDiS) & Centro Estudios Moleculares de la Celula, Facultad Ciencias Quimicas y Farmaceuticas & Facultad Medicina, Universidad de Chile, Santiago, Chile (S.L.); and the Department of Molecular Biology, University of Texas Southwestern Medical Center, Dallas (J.A.H.).

The online-only Data Supplement is available with this article at http://circ.ahajournals.org/lookup/suppl/doi:10.1161/CIRCULATIONAHA.113.002416/-/DC1.

Correspondence to Joseph A. Hill, MD, PhD, Division of Cardiology, University of Texas Southwestern Medical Center, NB11.200, 6000 Harry Hines Blvd, Dallas, TX 75390-8573. E-mail joseph.hill@utsouthwestern.edu

oxygen and nutrients to the injured tissue, triggers a complex cascade of events and a second wave of injury.[6] Indeed, reperfusion injury is a major contributor to infarct size, approaching 50% of total injury burden.[7] To address this problem, several small clinical trials have evaluated therapies such as ischemic postconditioning, cyclosporine, and hypothermia, and some have demonstrated protective effects.[8] However, as yet, no standard therapy exists, and an effective and clinically feasible therapy to mitigate reperfusion injury is sorely needed.

Many proteins are regulated by reversible acetylation of ε-amino groups on lysine residues. Appreciated first in the case of histone proteins, where acetylation leads to chromatin relaxation and access of transcriptional activators to DNA,[9] this widespread posttranslational modification occurs on numerous proteins beyond just histones. Reversible protein acetylation is governed by enzymes that attach (histone acetyltransferases) or remove (histone deacetylases, HDACs) acetyl groups. In the case of the latter, small-molecule inhibitors of HDACs are currently being tested for a variety of oncological indications. In mammalian cells, 18 HDACs have been described, grouped into 4 classes.[10] Gene deletion and overexpression studies have revealed important functions of several of these enzymes in pathological cardiac remodeling, including ventricular hypertrophy, apoptosis, necrosis, metabolism, contractility, and fibrosis.[11,12]

A series of preclinical studies, including those from our laboratory, have demonstrated potent cardioprotective benefits of HDAC inhibitors in murine models of myocardial stress, including ischemia/reperfusion (I/R).[13–16] Trichostatin A (TSA), an HDAC inhibitor specific to class I and II HDACs, reduces myocardial infarct size up to 50%.[15,16] TSA or another HDAC inhibitor, Scriptaid, reduced infarct size and preserved systolic function. Of note, HDAC inhibitor delivery as late as 1 hour after the ischemic insult still reduced infarct size to an extent similar to pretreatment.[16] These exciting results suggest that HDAC inhibition may be suitable to treat patients presenting with myocardial infarction at the time of percutaneous coronary intervention in the cardiac catheterization laboratory. However, recent evidence has unveiled surprisingly large differences in the disease mechanisms in murine models of disease relative to the human case.[17] These facts, coupled with the fact that an HDAC inhibitor that is structurally similar to TSA, suberoylanilide hydroxamic acid (SAHA; vorinostat), is approved by the US Food and Drug Administration (FDA) for the treatment of cutaneous T-cell lymphoma, led us to test SAHA's efficacy in a large-animal model of I/R.

Materials and Methods

Mouse Model of I/R

Eight- to 12-week-old C57BL6 wild-type mice were anesthetized with 2.4% isoflurane and placed in a supine position on a heating pad (37°C). Animals were intubated with a 19G stump needle and ventilated with room air with the use of a MiniVent mouse ventilator (Hugo Sachs Elektronik; stroke volume, 250 μL; respiratory rate, 210 breaths per minute). Following left thoracotomy between the fourth and fifth ribs, the left anterior descending coronary artery was visualized under a microscope and ligated by using a 6-0 Prolene suture. Regional ischemia was confirmed by visual inspection under a dissecting microscope (Leica) of the discoloration of the myocardium distal to the occlusion. For I/R, the ligation was released after 45 minutes of ischemia, and the tissue was allowed to reperfuse as confirmed by visual inspection. Sham-operated animals underwent the same procedure without occlusion of the left anterior descending coronary artery. All procedures were approved by the University of Texas Southwestern Medical Center Institutional Animal Care and Use Committee.

Rabbit I/R Protocol

Rabbits (6–8 lb male New Zealand White; Provance) were anesthetized with ketamine (40 mg/kg) plus xylazine (5 mg/kg). The animal was intubated and placed on mechanical ventilation. Fur was removed over the site of the incision and disinfected with surgical iodine. The animal was draped with sterile drapes. A warming light and Bair Hugger were used to maintain body temperature within a range of 35 to 37°C. Thoracotomy was performed via the fourth intercostal space. The circumflex artery was located and ligated with suture material (4-0 silk) attached to a nontraumatic needle. This snare was tightened to occlude the artery for 30 minutes (ischemia). The snare was then released, and reperfusion was confirmed visually. The retractor was removed and the lung was reinflated. The chest was then closed with 2-0 PDS suture, and the muscles and skin were closed by layer using 3-0 PDS absorbable suture and tissue adhesive, respectively. The animals were observed during recovery from anesthesia. After surgery, rabbits were treated with buprenorphine 0.05 mg/kg and, if necessary, once again the next morning for analgesia. Pain was assessed by signs of discomfort, lethargy, or anorexia. Twenty-four hours after reperfusion, rabbits were reanesthetized with ketamine (40 mg/kg) plus xylazine (5 mg/kg). The deeply anesthetized animals were then euthanized with 20 to 60 mg/kg sodium pentobarbitol. The heart was then excised with the ascending aorta preserved for cannulation. All procedures were approved by the University of Texas Southwestern Medical Center Institutional Animal Care and Use Committee.

For protein and imaging studies, ischemia was imposed for 30 minutes followed by 2 hours of reperfusion. After euthanization, the rabbit hearts were perfused with a 5% solution of phthalo blue dye (Heucotech, Fairless Hill, PA) in normal saline to delineate the area at risk and remote zone. One set of animals was used for protein study (4 animals per group). The heart was divided into 3 tissue zones: infarct zone (2–3 mm inside the line of blue dye), remote zone (2–3 mm outside the line of blue dye), and border zone (the remainder of the LV after removal of infarct and remote zones). Each zone of tissue was minced into small pieces, divided equally into 3 tubes, and flash frozen for subsequent Western blot analysis. Another set of animals (3 per group) was used for electron microscopy and terminal deoxynucleotidyl transferase dUTP nick end labeling (TUNEL) analyses.

2,3,5-Triphenyltetrazolium Chloride Staining

At the time of anesthesia and before euthanization, rabbits were given heparin 1000 U/kg for anticoagulation to ensure that the dye perfused well. The heart was excised and perfused with phosphate-buffered saline solution (5 mL) through an aortic cannula (fitted with a suture to close the aorta around the cannula). To delineate the occluded-reperfused coronary vascular bed, the coronary artery was then tied at the site of the previous occlusion, and the aortic root was perfused with a 5% solution of phthalo blue dye in normal saline (5 mL over 5 minutes). With the use of this procedure, the portion of the LV supplied by the previously occluded coronary artery (area at risk) was identified by the absence of blue dye, whereas the rest of the LV was stained dark blue.

To harvest samples for molecular biological analysis, hearts were cut in half and then 5 to 6 small samples (2 mm × 2 mm) were harvested by the use of scissors and forceps. Next, atrial and right ventricular tissues were excised. Then, the LV tissue was frozen and cut into 7 slices. To delineate infarcted from viable myocardium, the heart slices were incubated with 1% solution of 2,3,5-triphenyltetrazolium chloride in phosphate buffer (pH 7.4 at 37°C (50 mL per heart) for 40 minutes. The heart slices were then fixed in 10% neutral buffered formaldehyde, and, 24 hours later, they were weighed and photographed digitally. With this procedure, the nonischemic portion of the LV was stained dark blue, viable tissue within the region at risk was stained bright red, and infarcted tissue was white or light yellow.

The images were analyzed using ImageJ, and from these measurements the infarct size was calculated as a percentage of the region at risk using a weight-based method.

Measurement of Autophagic Flux in Mice

Mice harboring an RFP-GFP-LC3 transgene driven by a CAG promoter were generated. Mice were randomly assigned to 3 groups. One group received vehicle, dimethyl sulfoxide (DMSO), as control; one group received the SAHA pretreatment protocol (50 mg/kg SQ ×4); and the last group received the SAHA reperfusion protocol (100 mg/kg SQ ×1). The mice were subjected to 45 minutes of ischemia and 2 hours of reperfusion. Green fluorescent protein (GFP) and red fluorescent protein (RFP) signals were detected in frozen sections by confocal microscopy.

Measurement of Plasma SAHA Concentration

One hundred microliters of plasma was mixed with 200 μL of acetonitrile (containing 0.15% formic acid, 300 ng/mL benzylbenzamide as internal standard). The samples were vortexed for 15 s, incubated at room temperature for 10 minutes, and spun twice at 13 200 rpm in a standard microcentrifuge. The supernatant was then analyzed by liquid chromatography-tandem mass spectrometry. Buffer A: Water + 0.1% formic acid; Buffer B: MeOH + 0.1% formic acid; flow rate, 1.5 mL/min; column Agilent C18 XDB column, 5 μm packing 50 × 4.6 mm size; 0 to 1 minute 95% A, 1 to 1.5 minutes gradient to 95% B; 1.5 to 2.5 minutes 100% B, 2.5 to 2.6 minutes gradient to 95% A; 2.6 to 3.5 minutes 95% A; Internal Standard *N*-benzylbenzamide (transition from 212.1 to 91.1); compound transition, 265.1 to 232.021.

Primary Culture of Neonatal Rat Ventricular Myocytes

In brief, LVs from 1- to 2-day-old Sprague-Dawley rats were collected and digested with collagenase. The resulting cell suspension was preplated to clear fibroblasts. We then plated the cells at a density of 1250 cells per 1 mm^2 in medium containing 10% fetal bovine serum with 100 μmol/L bromodeoxyuridine. Typical cultures were notable for >95% cardiomyocytes.

Isolation and Culture of Primary Adult Rat Ventricular Myocytes

Adult rat ventricular myocytes (ARVMs) were isolated from hearts of male adult Sprague-Dawley rats (250–350 g). Rats were anesthetized with pentobarbital (intraperitoneally), hearts were removed, washed with Gerard buffer (0.19 mmol/L NaH_2PO_4, 1.01 mmol/L Na_2HPO_4, 10 mmol/L HEPES, 128 mmol/L NaCl, 4 mmol/L KCl, 1.4 mmol/L $MgSO_4$, 5.5 mmol/L glucose, 2 mmol/L pyruvic acid [pH 7.4]) and retroperfused (5 mL/min) with 2 mmol/L $CaCl_2$-containing Gerard buffer for 5 minutes, followed by 2 mmol/L EGTA-containing Gerard buffer for 1 minute, and finally with 0.12% (wt/vol) collagenase A (Roche)–containing Gerard buffer (digestion solution) for 30 minutes. Digested hearts were mechanically shattered in 20 mL of digestion solution and incubated at 37°C with constant agitation for 10 minutes, and supernatants were centrifuged at 500 rpm for 30 s. Remaining tissue was further digested with 20 mL of digestion solution. Pellets containing cardiac myocytes were washed in Gerard buffer and then resuspended in plating medium (Dulbecco's modified Eagle's medium supplemented with 5% fetal bovine serum, 1×Insulin-Transferrin-Selenium [41400-045, Invitrogen], 10 mmol/L 2,3-butanedione monoxime, and 100 U/mL penicillin-streptomycin). After calcium was reintroduced, cardiac myocytes were plated at a final density of $1.0\times10^3/mm^2$ on laminin-precoated culture dishes or coverslips. Culture medium (Dulbecco's modified Eagle's medium supplemented with 1×Insulin-Transferrin-Selenium [41400-045, Invitrogen], 10 mmol/L 2,3-butanedione monoxime and 100 U/mL penicillin-streptomycin) was replaced 4 hours later.

Simulated I/R in Cultured Cells and Cell Death Assay

For simulated ischemia/reperfusion (sI/R) neonatal rat ventricular myocyte (NRVM) studies, ischemia was imposed by a buffer exchange to ischemia-mimetic solution (in mmol/L: 20 deoxyglucose, 125 NaCl, 8 KCl, 1.2 KH_2PO_4, 1.25 $MgSO_4$, 1.2 $CaCl_2$, 6.25 $NaHCO_3$, 5 sodium lactate, 20 HEPES, pH 6.6) and placing the culture plates within a humidified gas chamber equilibrated with 95% N_2, 5% CO_2. After 2 to 5 hours of simulated ischemia, reperfusion was initiated by buffer exchange to normoxic NRVM culture medium with 10% fetal bovine serum and incubation in 95% room air, 5% CO_2. Controls incubated in normoxic NRVM culture medium with 10% fetal bovine serum were prepared in parallel for each condition. Cell death was detected by using the CytoTox 96 Non-Radioactive Cytotoxicity Assay (G1781, Promega).

For ARVMs, 2 μmol/L SAHA or DMSO was added 12 hours before sI/R in the control group and the group receiving 2 hours of ischemia (pretreatment). Then, 2 μmol/L SAHA or DMSO was added at reperfusion for a total of 2 hours of treatment in the group in which cells were treated with sI/R of 2 hours of ischemia and 2 hours of reperfusion. LC3 Western blots were performed to assay autophagic flux. ARVM cell death was evaluated by microscopy. Each group was studied in triplicate, and 2 representative views were examined for each sample. With 4 repeats, each group comprised a total 24 readings.

Reagents

Antibodies for immunoblotting were as follows: rabbit anti-LC3 was prepared in our laboratory based on synthetic peptides. GAPDH antibody was from Santa Cruz Biotechnology (Santa Cruz, CA), and ATG7 antibody was from Anaspec (54231) ATG5 antibody was from Abcam (ab108327) and cleaved caspase-3 antibody was from Cell Signaling (#9664). TSA was purchased from Biomol (Plymouth Meeting, PA). SAHA and bafilomycin A were purchased from LC Laboratory.

siRNA Knockdown

NRVMs were isolated and seeded at a density of 1.2 million/well in a 6-well dish. Twenty-four hours after plating, cardiomyocytes were incubated with small interfering RNA (siRNA) negative control (Neg, SIC001), siRNAs targeting ATG7 (top 2 rankings against rat, SASI_Rn01_00050326 and SASI_Rn01_00050327), or siRNAs targeting ATG5 (SASI_Rn01_00094887 and SASI_Rn01_00094888), each from Sigma and used according to the manufacturer's recommended protocols. In brief, siRNAs were reconstituted into a 40 mmol/L stock solution. Three microliters of the siRNA stock and 3 μL of RNAiMax transfectant were mixed together in 1 mL of Opti-MEM medium. Cardiomyocytes were incubated with the RNAiMax for 6 hours, followed by the addition of 1 mL of culture medium containing 20% serum. Twenty-four hours after the siRNA incubation, the cardiomyocytes were treated with SAHA at 2 mmol/L (overnight). Then, the cells were subjected to ischemia (5 hours) and reperfusion (1.5 hours) for cell death assay.

Electron Microscopy

Hearts were retrograde perfused by using phosphate-buffered saline and 2% glutaraldehyde in 0.1 mol/L cacodylate buffer. Postfixation occurred in 2% osmium tetroxide in 0.1 mol/L cacodylate buffer and 1% aqueous uranyl acetate, each for 1 hour. An ascending series of ethanol washes (50%, 70%, 90%, 100%) was performed, followed by transitioning to propylene oxide and then a 1:1 mixture of propylene oxide and EMbed 812 (Electron Microscopy Sciences). The tissue was incubated in EMbed for 1 hour, then placed in a 70°C oven to polymerize. Sections (75–80 nm) were cut by using a Leica ultramicrotome and a Diatome diamond knife, collected on 200-mesh copper grids, and post-stained with 5% uranyl acetate in ethanol (10 minutes) and Reynold lead citrate (5 minutes). A JEOL 1200 EX transmission electron microscope, operating at 40 to 120 kV and equipped with a digital camera, was used to image the sections.

Adenoviral Infection of Cultured Cardiomyocytes

NRVMs were plated as above on coverslips. Twenty-four hours after plating, cells were infected with adenovirus expressing GFP-LC3 (multiplicity of infection 10). After the cells were treated with SAHA or DMSO overnight, they were fixed with 4% paraformaldehyde and examined by confocal fluorescence microscopy.

Immunoblot Analysis

Protein lysates were separated by SDS/PAGE, transferred to Hybond-C nitrocellulose membrane (HYBOND-ECL Nitrocellulose), and subjected to immunoblot analysis.

TUNEL Staining

TUNEL staining was performed with the use of the In Situ Cell Death Detection kit (Roche) according to the manufacturer's instructions. Propidium iodide staining was performed to visualize nuclei after TUNEL reaction, and the percentage of TUNEL-positive nuclei was quantified using ImageJ software. To overlay the striated muscle fiber with TUNEL signals, a differential interference contrast microscopy image was taken at 400× magnification.

Echocardiography

Echocardiograms were performed on anesthetized rabbits (ketamine 40 mg/kg plus xylazine 5 mg/kg) with the use of an Acuson Sequoia C512 (software Sequoia 9.51) system and a 15L8 Acuson linear probe. A short-axis view of the LV at the level of the papillary muscles was obtained, and M-mode recordings were obtained from this view. Left ventricular internal diameter at end-diastole (LVIDd) and end-systole (LVIDs) were measured from M-mode recordings. Fractional shortening was calculated as (LVIDd − LVIDs)/LVIDd (%).

Mouse echocardiograms were performed on conscious, gently restrained mice using a Vevo 2100 system and an 18-MHz linear probe. A short-axis view of the LV at the level of the papillary muscles was obtained, and M-mode recordings were obtained from this view. Fractional shortening was calculated using the same approach as in rabbit.

Statistical Methods

Averaged data are reported as mean±standard error of the mean. Data were analyzed with the unpaired Student *t* test for 2 independent groups, paired *t* test for dependent data, and the 1-way analysis of variance followed by the Tukey post hoc test for pairwise comparisons. Studies with repeat measures were analyzed using repeated-measures analysis of variance. For all statistical tests, a P value of <0.05 was considered statistically significant, and all tests were 2-tailed. For animal studies (both mouse and rabbit data), normality tests were assessed via the Shapiro-Wilk and Anderson-Darling statistics. As normality was confirmed (Table I in the online-only Data Supplement), results were presented from parametric statistics. In the case of nonnormality, nonparametric tests were used (Mann-Whitney *U* test for 2-group comparisons and the Kruskal-Wallis test for ≥3 groups followed by the Dunn test to correct for multiple comparisons). To be most stringent, all animal data and statistical comparisons were verified using nonparametric methods regardless of passing normality tests (Table II in the online-only Data Supplement). All statistical analyses were performed using GraphPad Prism (version 6.01) software.

Results

TSA and SAHA Reduce Infarct Size and Preserve Systolic Function in Mouse I/R

TSA has been previously reported to reduce infarct size ≈50% in an ex vivo Langendoff model and an in vivo mouse model of I/R.[15,16] To verify and extend these findings, we treated C57BL6 mice with TSA 1 mg/kg IP 1 day before in vivo I/R (ischemia 45 minutes and reperfusion 24 hours). Infarct size and area at risk for infarction were determined by 2,3,5-triphenyltetrazolium chloride staining (Figure1A). TSA reduced infarct size, normalized to area at risk, by ≈50%, a result comparable to earlier studies (Figure 1B).[15,16] There was no significant difference in the area at risk between the 2 groups (Figure 1C), confirming that the surgical injury was equivalent between treatment groups. Similar findings emerged when infarct size was normalized to LV weight, which was reduced by ≈50% (Figure 1D).

Echocardiography was performed in mice injected daily with TSA (1 day, 3 days, 1 week, 2 weeks) following surgery to evaluate ventricular size and systolic function. These data revealed significant TSA-dependent protection (Figure 1B and 1D), which persisted through the entire 2-week observation period (Figure 1E).

We next set out to determine whether SAHA, an FDA-approved hydroxamic acid–based compound structurally similar to TSA with similar HDAC isoform specificity, afforded similar benefits. SAHA has an IC_{50} 30 to 50 times greater than that of TSA and different pharmacokinetics.[18,19] We therefore tested 2 doses of SAHA, 30 mg/kg and 50 mg/kg, which are within the range of the doses used in cancer studies.[20–22] We followed a pretreatment protocol, in which mice received SAHA subcutaneously every12 hours 1 day before surgery (2 doses), a third dose one-half hour before surgery,

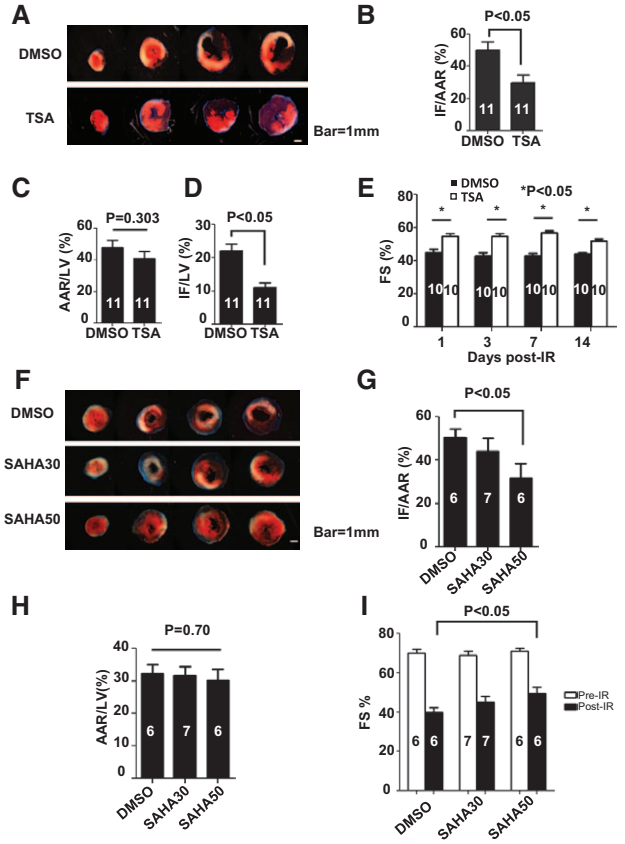

Figure 1. TSA and SAHA reduce infarct size and preserve systolic function in mouse I/R. **A,** Representative TTC staining of TSA and DMSO pretreatment groups after I/R (45 minutes/24 hours). White indicates infarct; red, AAR; and blue, remote. **B,** TSA reduced infarct (IF) size normalized to AAR (n=11, $P<0.05$) as determined by TTC staining after I/R. **C,** There were no significant differences in AAR among groups. **D,** TSA reduced IF normalized to left ventricle weight (LV; n=11, $P<0.05$). **E,** TSA daily injection for up to total 14 days treatment improved systolic function measured as %FS after I/R (n =10, $P<0.05$). **F,** Representative TTC staining of SAHA and DMSO pretreatment groups after I/R (45 minutes/24 hours) **G,** SAHA pretreatment before I/R (50 mg/kg, SAHA50) reduced IF/AAR significantly (n=6–7, $P<0.05$). SAHA at a lower dose (30 mg/kg, SAHA30) did not achieve statistical significance. **H,** There were no significant differences in AAR among groups. **I,** SAHA50 treatment partially preserved %FS measured by echocardiography after I/R (n=6–7, $P<0.05$). AAR indicates area at risk; DMSO, dimethyl sulfoxide; FS, fractional shortening; IF, infarct; I/R, ischemia/reperfusion; SAHA, suberoylanilide hydroxamic acid; TSA, trichostatin A; and TTC, 2,3,5-triphenyltetrazolium chloride.

and a fourth dose at the time of reperfusion. Throughout, the surgeon, echocardiographer, and 2,3,5-triphenyltetrazolium chloride staining interpreter were blinded to treatment group assignments. SAHA (50 mg/kg) reduced infarct size by ≈45% (P<0.05; Figure 1F and 1G). Lower-dose SAHA (30 mg/kg) manifested a trend toward reduced infarct size (≈20%) that failed to achieve statistical significance. We observed no difference in area at risk across all the groups (Figure 1H). Echocardiographic analysis demonstrated that SAHA treatment (50 mg/kg) partially preserved systolic function after I/R (percent fractional shortening [%FS] increased from 40±2% to 50±3%, P<0.05, n=6–7; Figure 1I). In aggregate, these data establish that SAHA is functionally similar to TSA in its ability to blunt I/R damage in mice.

SAHA Reduces Infarct Size and Preserves Systolic Function in Rabbit I/R

In some instances, the human response to disease-related stress differs substantially from that observed in murine models,[17] emphasizing the critical importance of testing in large animals before moving to humans. With a vision toward translating our findings to the clinical context, we tested the effects of SAHA in I/R injury in a large-animal model. Given that rabbits metabolize SAHA ≈3-fold faster than mice,[19] we tested a range of doses to identify an optimal dose (Figure IA in the online-only Data Supplement). We also devoted considerable effort to carefully mapping the coronary anatomy in the rabbit, which is known to be highly variable,[23] to achieve a stable area at risk (Figure IB in the online-only Data Supplement).

Rabbits were randomly assigned among 3 treatment arms (Figure 2). In 1 arm (pretreatment), rabbits received SAHA 150 mg/kg SQ every 12 hours 1 day before surgery (2 doses), a third dose at one-half hour before surgery, and a fourth dose at the time of reperfusion. In the second treatment arm (reperfusion-only), animals received 2 doses of vehicle (DMSO) before surgery and a single dose of SAHA at 300 mg/kg at the time of reperfusion. Finally, the third arm (control) received vehicle injections for all 4 injection times. Animals were randomly assigned to 1 of 3 treatment groups by a single investigator, who was the only investigator aware of treatment assignment.

Both the pretreatment and reperfusion-only treatment arms manifested significantly reduced infarct size normalized to area at risk (28±4%, 34±4%, respectively) in comparison with the control arm (50±2%; Figure 3A and 3B). There were no differences in area at risk across the 3 groups, confirming that the surgical procedures were similar (Figure 3C). Infarct size normalized to LV weight also manifested significant reduction (P<0.05, n=7) in both the pretreatment (8.1±2%) and reperfusion-only (10.4±1%) treatment arms in comparison with control (15±1%; Figure 3D).

Echocardiography was performed, and the %FS was measured as an index of cardiac function, both before and after I/R. Baseline echocardiographic analysis of ventricular function revealed no significant differences among treatment groups before I/R. Measurements obtained 24 hours after surgery demonstrated a decrease in %FS from 33.5±0.6% to 19±0.5% (P<0.001, n=7) in the control group (Figure 3E and 3F). This decrease in systolic function was mitigated by

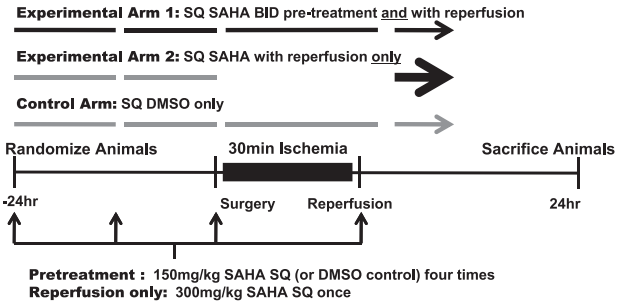

Figure 2. Experimental design testing SAHA's cardioprotective effects. Experimental Arm 1: The pretreatment group received SAHA 150 mg/kg SQ every 12 hours one day before the surgery, 1 dose one-half hour before surgery, and 1 dose at the time of reperfusion. Experimental Arm 2: The reperfusion-only group received 2 doses of vehicle (DMSO) 1 day before surgery and 1 dose of SAHA (300 mg/kg) at the time of reperfusion. Control Arm: The control group received only 4 doses of DMSO, the vehicle used for SAHA. BID indicates twice daily; DMSO, dimethyl sulfoxide; SAHA, suberoylanilide hydroxamic acid; and SQ, subcutaneously.

SAHA treatment, regardless of whether the drug was administered before surgery (%FS declined from 34.7±0.5 to 26±1%, P<0.001, n=7) or exclusively at reperfusion (%FS declined from 33.7±0.6 to 27±1%, P<0.001, n=7; Figure 3F).

Similar protective effects afforded by SAHA were observed in the preliminary experiments we performed to optimize the surgical I/R intervention. When this data set was combined with our blinded/randomized preclinical trial, the statistical significance was even more robust (Figure IC and ID in the online-only Data Supplement, nonrandomized; Figure IE through IH in the online-only Data Supplement, combined). These data provide strong evidence that SAHA blunts I/R-induced declines in infarct size and systolic function by ≈50% (Figure 3G).

SAHA Serum Concentrations Are Comparable to Human

As noted, the rate of SAHA metabolism in rabbits is substantially faster than in humans.[19] To establish a correlation between the SAHA serum concentrations effective in blunting I/R injury in rabbits with levels achievable clinically in humans, we measured SAHA serum levels. To determine the cumulative exposure to drug, we calculated the area under the curve (AUC) by measuring plasma SAHA concentrations at 15, 30, 60, 120, 240, 360, 480 minutes and 24 hours after a single dose of SAHA (300 mg/kg SQ). In 8 rabbits, the C_{max} was 3.3±0.4 μmol/L, time to peak concentration (T_{max}) was 1.0±0.5 hour, the 8-hour AUC was 12.7±1.3 μmol/L•h, and the 24-hour AUC was 20.6±2.0 μmol/L•h (Figure 4). In comparison, human subjects with T-cell lymphoma receiving a high-dose SAHA regimen (800 mg PO daily) achieved a C_{max} of 1.7±0.7 μmol/L and a median T_{max} of 2.1 (0.5–6 hours), with a mean AUC of 8.6±5.7 μmol/L•h. In other words, the pharmacokinetics and serum concentrations of SAHA achieved in our rabbit study, with drug delivered subcutaneously, exceed those seen in humans receiving dosing by mouth.[18] In 1 phase 1 clinical trial, patients received various doses of SAHA intravenously: 75, 150, 300, 600, and 900 600 mg/m^2 per day.[24]

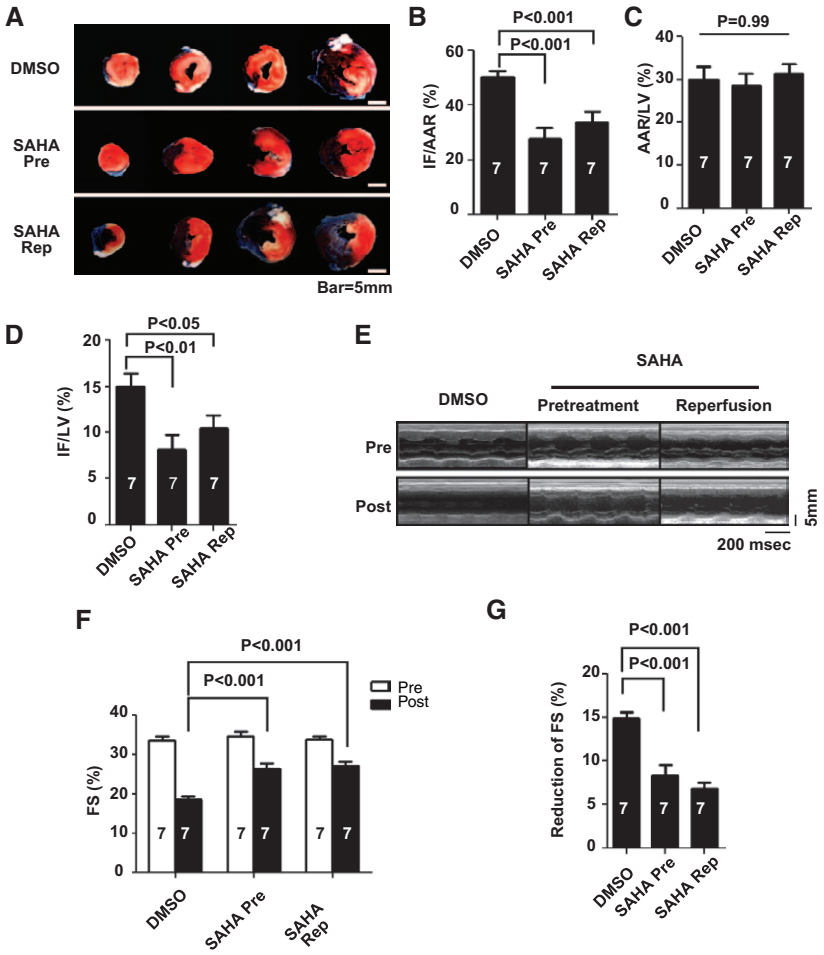

Figure 3. SAHA reduces infarct size and preserves systolic function in a rabbit I/R model. **A,** Representative TTC staining in 3 treatment groups after I/R (30 minutes/24 hours). White indicates infarct; red, AAR; and blue, remote. **B,** SAHA reduced IF/AAR as determined by TTC staining (n=7, *P*<0.001). **C,** There were no significant differences in AAR among groups. **D,** SAHA reduced IF normalized by left ventricle weight (LV; n=7, *P*<0.05). **E,** Representative M-mode echocardiograms. **F,** SAHA treatment partially preserved echocardiography-determined %FS after I/R (30 minutes/24 hours; n=7, *P*<0.001). **G,** The reduction in %FS after I/R was significantly lower in the SAHA treatment group (n=7, *P*<0.001). AAR indicates area at risk; DMSO, dimethyl sulfoxide; FS, fractional shortening; IF, infarct; I/R, ischemia/reperfusion; SAHA, suberoylanilide hydroxamic acid; TSA, trichostatin A; and TTC, 2,3,5-triphenyltetrazolium chloride.

By comparison with these data, the SAHA drug exposure in rabbit falls within the moderate-dose range (300–600 mg/m^2 per day; Table).[24] These data suggest that the drug exposure we achieved in rabbits is comparable to that observed in human subjects receiving either 2 doses of SAHA by mouth or an intravenous dose of SAHA.

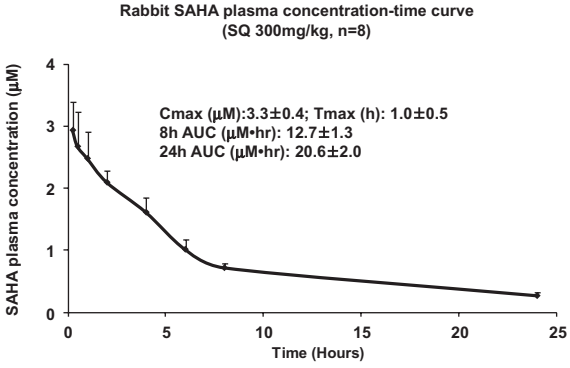

Figure 4. SAHA plasma concentration–time curve in rabbits receiving 300 mg/kg at the time of coronary reperfusion. Blood was collected at 15, 30, 60, 120, 240, 360, 480 minutes and 24 hours after a single dose of SAHA (300 mg/kg SQ) was administered at the time of reperfusion. In 8 rabbits, C_{max} was 3.3±0.4 μmol/L; T_{max} was1.0±0.5 hour; 8 hour AUC was 12.7±1.3μmol/L•h; 24 hour AUC was 20.6±2.0 μmol/L•h. AUC indicates area under the curve; SAHA, suberoylanilide hydroxamic acid; and SQ, subcutaneously.

SAHA Increases Autophagy in the Infarct Border Zone

Autophagy is an evolutionarily conserved cellular process in which the cell isolates, degrades, and recycles portions of the cytoplasm, including damaged organelles. Alterations in autophagic activity have been linked to a variety of pathological conditions and can be either adaptive or maladaptive, depending on the context.[25] Autophagy has been recognized to be involved in reperfusion injury.[26] By replenishing energy stores during ischemia and removing damaged mitochondria, autophagy can act to protect the cardiomyocyte from damage that might lead to cell death.[26] SAHA has been shown to increase autophagy in cancer cells.[27] To assess the role of

Table. Comparison of Plasma SAHA Levels in Rabbit With Those of Human Subjects Receiving IV SAHA

Dose Level	n	C_{max}, ng/mL	AUC_{inf}, h × ng/mL
300 mg/m^2	11	2646±588	4285±1150
300 mg/kg SQ rabbit	8	872±106	5438±528
600 mg/m^2	9	6334±3086	11 233±6928
900 mg/m^2	11	9525±1611	16 611±4533

Measured rabbit plasma SAHA concentration parameters were compared with those from human subjects receiving IV SAHA during a phase 1 clinical trial. AUC indicates area under the curve; IV, intravenous; SAHA, suberoylanilide hydroxamic acid; and SQ, subcutaneous.

autophagy in the cardioprotective effect of SAHA in I/R, we randomly assigned 16 rabbits and treated them with either SAHA (300 mg/kg SQ at reperfusion) or vehicle (DMSO). The animals were euthanized 2 hours after reperfusion, and the hearts isolated and analyzed as 3 distinct zones: a remote zone distant from the ischemic area, an infarct zone within the center of the area perfused by the ligated artery, and a border zone that surrounded the site of infarction (Figure 5A).

Autophagy was evaluated initially by Western blot detection of the autophagosome-associated lipidated isoform of LC3 (LC3-II). LC3-II levels, reflective of autophagosome abundance, were similar in the infarct, remote, and border zones of hearts of the vehicle-treated group. By contrast, significant increases in LC3-II levels were detected in the border zone of hearts in the SAHA treatment arm in comparison with the infarct or remote zones (Figure 5B). Autophagosome accumulation in the infarct border zone of SAHA-treated hearts was verified by electron microscopy (Figure 5C). Also, consistent with a decrease in infarct size, apoptosis (measured by TUNEL assay and cleaved caspase-3) was decreased within the infarct border zone of SAHA-treated rabbits (Figures II and III in the online-only Data Supplement).

Autophagy is a dynamic process of flux. As such, increased steady-state levels of autophagosomes can signify either an increase of autophagy, a block in downstream lysosomal processing of these autophagosomes, or both. We therefore assayed autophagic flux, or autophagosome biogenesis, maturation, and lysosomal degradation, using mice that we engineered to harbor an RFP-GFP-LC3 transgene driven by a CAG promoter. Yellow puncta, reflective of combined GFP and RFP fluorescence, mark autophagosomes, whereas red puncta (RFP only) mark autolysosomes whose acidic pH quenches GFP fluorescence. Under conditions where flux is blocked, an increase in yellow signal is observed with little increase in the red signal. Mice were subjected to 45 minutes of ischemia and 2 hours of reperfusion, and GFP and RFP signals were detected in frozen sections. In the infarct border zone of SAHA-treated mice (using either the pretreatment protocol; 50 mg/kg SQ ×4 or the reperfusion-only protocol; 100 mg/kg SQ once at the time of reperfusion), both GFP/RFP and RFP signals were significantly increased, indicating increased incorporation of LC3 into both autophagosomes and autolysosomes (Figure 5D). These data, then, suggest that the accumulation of autophagosomes observed in the infarct border zone of SAHA-treated rabbits derives from a bona fide increase in autophagic flux.

SAHA's Cardioprotective Effects Are Dependent on Autophagic Flux

To examine whether increases in autophagic flux contribute to the cardioprotective effects of SAHA, we turned to an in vitro assay of sI/R. NRVMs were treated with SAHA or vehicle overnight and then subjected to 5 hours of simulated ischemia followed by 1.5 hours of simulated reperfusion. We first examined cell death by measuring lactate dehydrogenase levels in the culture medium. Exposure of NRVMs to sI/R resulted in a >4-fold increase in cell death (Figure 6A). SAHA treatment, however, elicited a significant decrease in sI/R-induced cell death. These results are consistent with the in vivo cardioprotective properties of SAHA (Figure 6A).

To examine autophagic activation preceding cell death, NRVMs were exposed to sI/R (2 hours of ischemia only or 2 hours of ischemia and 2 hours of reperfusion) in the presence/absence of SAHA. Of note, we selected 2-hour ischemia instead of 5-hour ischemia in the cell death assays to focus on early molecular processes preceding cell death. Steady-state levels of LC3-II were slightly decreased during both the ischemic and reperfusion stages of injury. These decreases correlated with a decrease in autophagic flux as demonstrated by decreased levels of LC3-II observed after blocking lysosomal activity with bafilomycin A. In the absence of bafilomycin A, LC3-II levels were similar in both vehicle and SAHA treatment groups; however, lysosomal inhibition by bafilomycin A uncovered a dramatic increase in autophagic flux induced by SAHA, as evidenced by significant accumulation of LC3-II (Figure 6B). We confirmed this activation of autophagic flux by SAHA using an LC3-GFP adenovirus. NRVMs treated with SAHA manifested a noticeable increase in LC3-GFP puncta formation in comparison with the DMSO control (Figure 6C). This increase was similar to that observed with the established autophagy inducer rapamycin (Figure 6C).

Induction of autophagic flux by SAHA treatment both before sI/R and at reperfusion was also observed in ARVMs. Microscopic methods were used to detect ARVM cell death based on distinct morphological changes, an approach used previously to quantify I/R-induced ARVM cell death.[28,29] SAHA treatment at the time of reperfusion significantly attenuated sI/R-induced cell death, suggesting that this cardioprotective effect is not specific to neonatal cells (Figures IV and V in the online-only Data Supplement).

Having established that SAHA induces autophagic flux and decreases sI/R-induced cell death, we next examined whether this increased autophagy was required for the protection we observed. The effect of SAHA on cell survival was measured in the presence of siRNA targeting each of 2 essential autophagy proteins, ATG7 or ATG5. Again, SAHA treatment protected NRVMs from sI/R-induced cell death. However, knockdown of either ATG7 or ATG5 abolished the protective effect of SAHA (Figure 6D and Figure VIA in the online-only Data Supplement). In each case, 2 sequence-independent siRNAs were tested to confirm specificity. Additionally, RNAi-dependent depletion of either ATG7 or ATG5 had no effect on the levels of the other protein (Figure 6E and Figure VIB in the online-only Data Supplement). These data, then, point to a critical requirement of autophagic flux in the cardioprotective actions of SAHA.

To mimic in vivo conditions of reperfusion-only treatment, we tested the effect of SAHA when added at the time of reperfusion during simulated I/R. Consistent with our findings with SAHA pretreatment, SAHA added at the time of simulated reperfusion induced autophagic flux in NRVM (Figure 7A) and increased NRVM survival (Figure 7B). This reperfusion-only cardioprotection also depended on autophagy, because knockdown of ATG7 resulted in a loss of the survival benefit of SAHA treatment (Figure 7B).

In our previous studies using a model of chronic pressure-overload hypertrophy, we showed that long-term treatment (7 days) with TSA led to a reduction in autophagic flux.[30] At face value, this seems to contradict the SAHA-induced

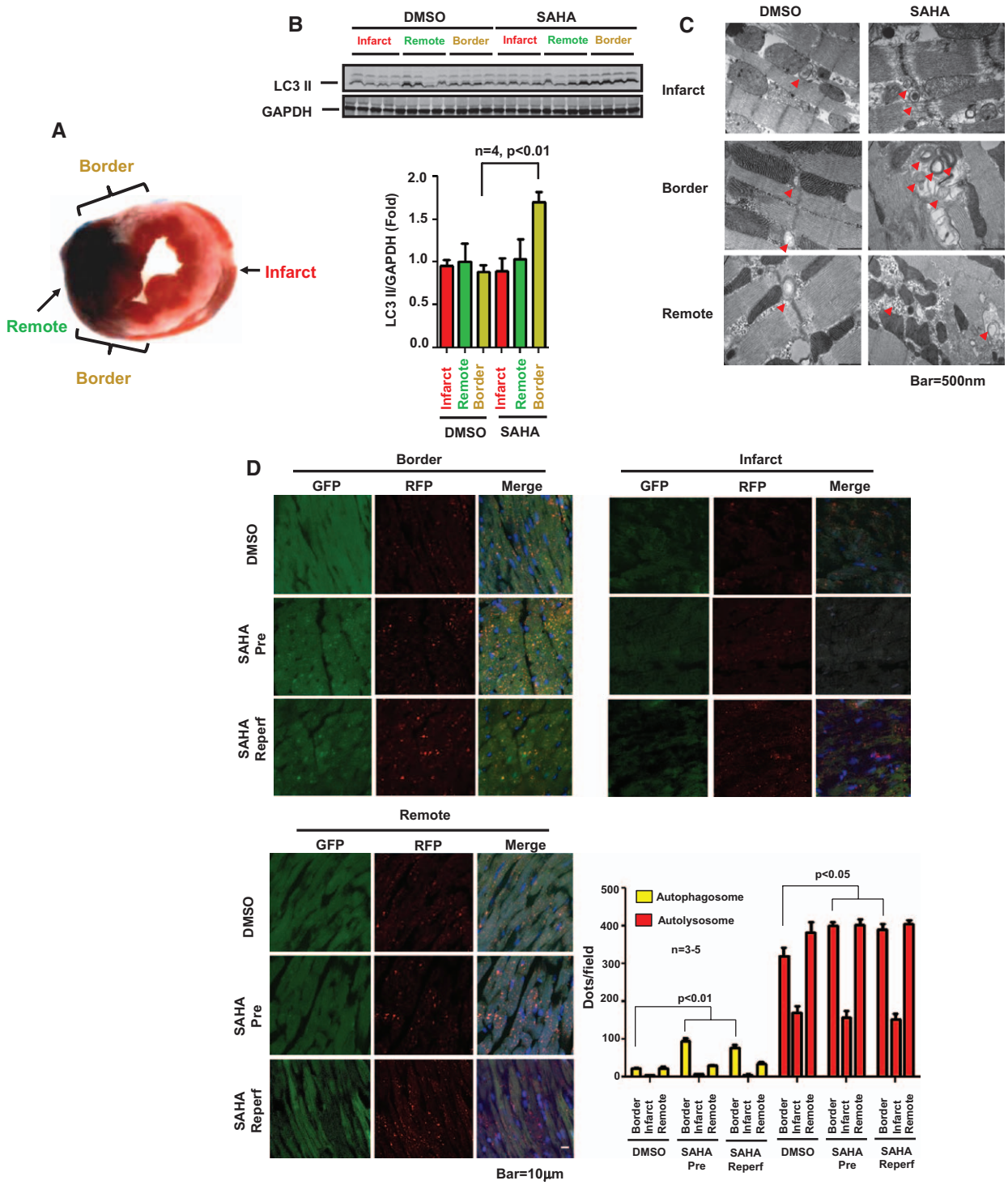

Figure 5. SAHA increases autophagic flux in the infarct border zone. **A,** Rabbit myocardium samples were harvested as depicted for Western blots and EM studies. Red indicates infarct zone; green, remote zone; and yellow, border zone. **B, Upper,** LC3 Western blot analysis of protein lysates harvested from the indicated tissue zone (I/R: 30 minutes/2 hours). SAHA was administered only at the time of reperfusion (reperfusion-only group). GAPDH is shown as loading control. **B, Lower**, Quantification. LC3-II normalized to GAPDH (n=4, $P<0.01$). **C,** EM images depicting double membrane autophagosomes. SAHA treatment increased autophagosomes significantly within the border zone (n=3) after I/R (30 minutes/2 hours). **D,** CAG-RFP-GFP-LC3 transgenic mice subjected to I/R (45 minutes/2 hours). Both yellow dots (autophagosomes) and red dots (autolysosomes) were significantly increased by SAHA treatment within the I/R border zone (n=3–5). $P<0.01$ and $P<0.05$, respectively. Quantification is shown in the graph at **bottom right**. Bar, 10 μm. DMSO indicates dimethyl sulfoxide; EM, electron microscopy; GFP, green fluorescent protein; Reperf, reperfusion; RFP, red fluorescent protein; and SAHA, suberoylanilide hydroxamic acid.

increases in autophagic flux seen here. However, autophagic flux was, in fact, downregulated in cultured NRVM treated with TSA in serum-free medium for 48 hours.[30] Given this, we reasoned that this apparent discrepancy may derive from differences in the conditions and duration of HDAC inhibition used in our 2 studies.

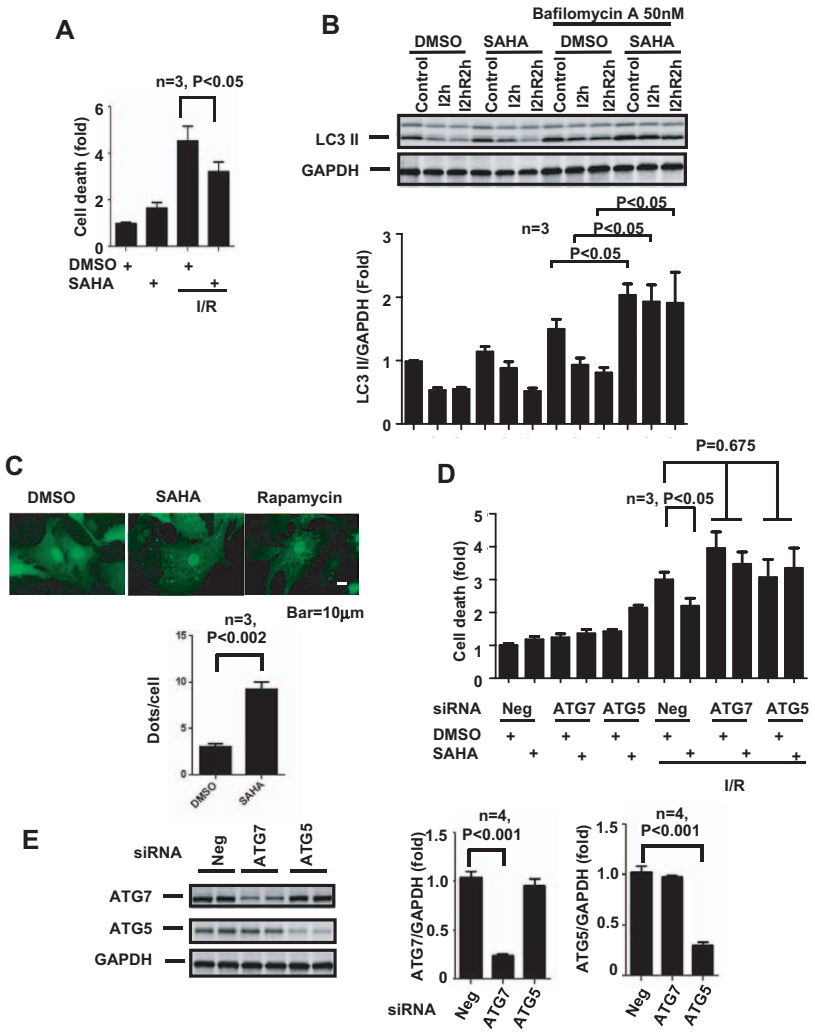

Figure 6. SAHA regulates autophagic flux during I/R, and SAHA's cardioprotective effects depend on autophagic flux. **A,** LDH cell death assay. SAHA treatment (2 μmol/L) reduced cell death ≈30% after simulated I/R (sI/R; 5 hours/1.5 hours; n=3, *P*<0.05). **B, Upper,** LC3 Western blot. At steady state, LC3-II levels normalized to GAPDH decreased in both DMSO and SAHA groups after 2 hours of ischemia (I2h) and 2 hours of ischemia plus 2 hours of reperfusion (I2hR2h). However, after bafilomycin A treatment, SAHA treatment induced increases in LC3-II levels even after simulated I/R (n=3, *P*<0.05). **B, Lower,** Quantification. **C,** Autophagic flux measurement with the use of adenovirus hosting GFP-LC3. SAHA treatment increased autophagic flux as evidenced by increased GFP-LC3 puncta signal. **D,** LDH cell death assay in the settings of ATG7 or ATG5 knockdown. Suppression of ATG7 and ATG5 both abolished SAHA's cardioprotective effects after sI/R (5 hours/1.5 hours; n=3, *P*<0.05). **E,** RNAi knockdown of ATG7 and ATG5. **Left,** Western blots. **Right,** quantification. DMSO indicates dimethyl sulfoxide; I/R, ischemia/reperfusion; LDH, lactate dehydrogenase; SAHA, suberoylanilide hydroxamic acid; and siRNA, small interfering RNA.

To test this directly, NRVMs were treated with TSA or SAHA in the presence/absence of bafilomycin A, and cells were collected over the course of 3 to 48 hours posttreatment. Western blot analysis demonstrated an increase in autophagic flux with TSA treatment that peaked at 12 hours and diminished significantly below baseline by 48 hours (Figure VII in the online-only Data Supplement). SAHA treatment manifested a similar pattern (Figure VII in the online-only Data Supplement). Thus, HDAC inhibition appears to elicit a time-dependent biphasic effect on autophagic flux.

Discussion

Ischemia/reperfusion is a major mechanism of injury in many forms of cardiovascular disease. In this setting, both the ischemic and reperfusion phases of the process confer harm to a roughly equivalent extent. Whereas many means of mitigating ischemic injury have emerged, constituting the standard-of-care in patients with coronary artery disease, no standard therapies are presently available to target reperfusion injury.

Recent work has uncovered a significant cardioprotective effect of HDAC inhibition in I/R injury.[15,16] These studies, which are remarkably concordant and emerge from independent laboratories, have relied on mouse models of I/R injury. Further, mechanisms underlying this benefit of HDAC inhibition remain obscure.

Here, we have extended these studies with a preclinical trial in a large-animal model. We have used rigorous methodology mimicking the methods typical of a clinical trial: prespecified end points and power calculations, randomization, and strict blinding of personnel. With this approach, we have uncovered robust cardioprotective effects of SAHA in rabbits. Further, preservation of contractile performance and the ≈40% decreases in infarct size were essentially equivalent when animals were pretreated with drug or when the drug was administered exclusively at the time of reperfusion. Our studies went on to identify an effect of SAHA to promote autophagic flux in cardiomyocytes within the infarct border zone, which was required for its cardioprotective activity. Finally, we demonstrate that SAHA-dependent activation of autophagic flux is required for the benefit.

HDAC Inhibition in I/R Injury

HDAC inhibition has been shown to blunt pathological changes in models of pressure overload.[14,30] Given this, HDAC inhibitors have also been tested in another prevalent form of pathological stress, cardiac ischemia.[31] In a rat model of myocardial infarction, the HDAC inhibitors valproic acid

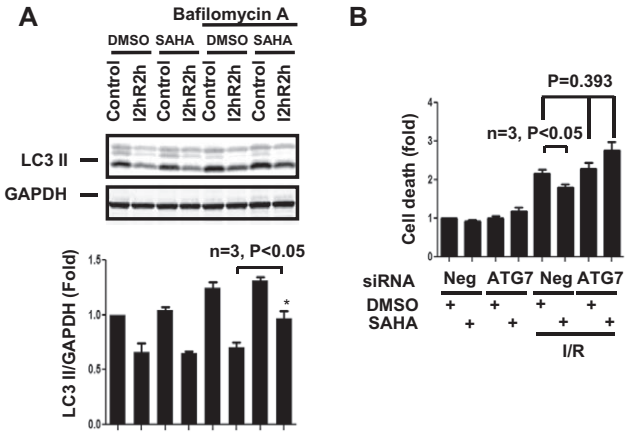

Figure 7. A, Upper, LC3 Western blot. At steady state, LC3-II levels normalized to GAPDH decreased in both DMSO and SAHA groups after 2 hours of ischemia plus 2 hours of reperfusion (I2hR2h). However, after bafilomycin A treatment, SAHA treatment induced increases in LC3-II levels after simulated I/R (sI/R, n=3, $P<0.05$). **Lower,** Quantification. **B,** LDH cell death assay. SAHA treatment (2 μmol/L) reduced cell death ≈20% after sI/R (5 hour/1.5 hour; n=3, $P<0.05$). Suppression of ATG7 abolished SAHA's cardioprotective effects after sI/R (n=3, $P<0.05$). DMSO indicates dimethyl sulfoxide; I/R, ischemia/reperfusion; LDH, lactate dehydrogenase; SAHA, suberoylanilide hydroxamic acid; and siRNA, small interfering RNA.

and tributyrin reduced cardiomyocyte hypertrophy and collagen deposition in both the remote and border zones of the infarcted LV.[32] Systolic function was also preserved. Finally, these protective effects were abolished by theophylline, an HDAC activator.[32]

Two studies tested HDAC inhibitors in murine I/R. With the use of an ex vivo Langendorff model, both perfusion of the explanted heart with TSA or treatment of the animal with TSA before surgery reduced infarct size and preserved systolic function.[15] TSA-induced p38 activation and acetylation of p38 at lysine residues were posited as underlying mechanisms.[15] Another study reported that HDAC activity increased significantly after cardiac I/R in vivo, and HDAC inhibition (TSA, Scriptaid) reduced infarct size and preserved systolic function.[16] Of note, administration of the HDAC inhibitor 1 hour after the ischemic insult reduced infarct size to an extent similar to that observed with pretreatment before surgical injury.[16] This study also reported that HDAC inhibition reduced hypoxia-inducible factor-1α levels, diminished vascular permeability, and diminished cell death.[16]

In a murine model of myocardial infarction, TSA stimulated c-kit+ cardiac stem cell proliferation.[33] In c-kit-null mice, TSA's beneficial effects were abolished, and reintroduction of TSA-treated wild-type c-kit+ cardiac stem cells into c-kit-null mice restored the beneficial remodeling effects of TSA.[33] After exposure to TSA, the abundance of c-kit+ cardiac stem cell–derived myocytes was significantly increased.[33] Together, these findings raise the possibility that HDAC inhibition could be used initially as an infarct size–reducing strategy and subsequently as long-term therapy to blunt postinfarct remodeling by mobilizing cardiac stem cells.

HDAC Inhibition in Myocardial I/R: Translating to the Human Case

We report here that SAHA confers robust cardioprotection in a large-animal model of myocardial I/R. These experiments were conducted in the context of 2 HDAC inhibitors, namely Zolinza (vorinostat, structurally similar to TSA) and Istodax (romidepsin), having received FDA approval for use in cutaneous T-cell lymphoma. Meanwhile, clinical trials with several others are underway in a number of tumor types. Given the pressing clinical need for drugs to treat I/R and the current availability of HDAC inhibitors approved for human use, we turned our attention to consideration of testing in humans.

It should be acknowledged that many agents targeting reperfusion injury have failed in clinical testing; why should SAHA be any different? Examination of those previous trials is instructive, revealing several reasons that could explain the failure.[8] In some cases, strategies tested in preclinical models did not manifest robust cardioprotective benefit. Many were not verified in multiple independent laboratories. Often, the tested agents were not administered at the time of reperfusion to mimic the clinical context. Many were not tested in a large-animal model. In some cases, protocols required of a rigorous clinical trial were not used.[8] In light of these failings, we have addressed each of these issues with data that are robust, reproducible across independent laboratories, and concordant across species. Further, benefits seen when the drug is delivered at reperfusion were similar to those seen when the animal is pretreated with drug.

In other words, SAHA fulfills the most stringent requirements for a successful antireperfusion injury agent in patients with myocardial infarction. HDAC inhibition has been demonstrated in at least 3 independent laboratories, including ours, to reduce infarct size robustly (≈50%) in a murine I/R model.[15,16] SAHA is available as an FDA-approved anticancer HDAC inhibitor with an acceptable safety profile.[24] In addition, we report here that SAHA reduces infarct size and preserves systolic function after I/R injury, delivered at reperfusion, in a large-animal model.

These findings suggest that SAHA has the potential to emerge as an antireperfusion injury therapeutic strategy. However, limitations should be acknowledged. Surgical ligation of a disease-free coronary artery is not equivalent to thrombotic occlusion of a diseased vessel in a patient with comorbidities. To address this concern rigorously, a pilot efficacy clinical trial in patients with ischemic heart disease is required.

SAHA's Plasma Concentration Is Achievable in Human Subjects

The metabolism of SAHA in rabbit differs from that in humans, being ≈3-fold more rapid.[19] Nevertheless, the C_{max} of SAHA in rabbit is similar to that observed in patients receiving oral therapy, and the 8-hour AUC is only 50% higher than that in humans. We believe that the high 24-hour AUC in rabbit is artificially prolonged, deriving from a depot effect of subcutaneous injection, as the plasma concentration has decreased below therapeutic levels 8 hours after injection (≈4 half-lives).[18] In addition, it is noteworthy that the AUCs measured in patients with cancer were obtained in the context of

multiple comorbidities and multiple drug exposures, likely provoking gastrointestinal disturbance, renal dysfunction, and a fasting state.[18] Thus, higher C_{max} and AUC might be achievable in patients with ST-segment elevation myocardial infarction, who are typically not fasted when presenting for percutaneous coronary intervention, using an 800 mg PO dose. Alternatively, 2 separate doses 1 hour apart could be administered. In any event, the AUC observed in rabbit is readily achievable in humans exposed to moderate doses delivered intravenously.[24]

Another issue is the safety of SAHA in patients with myocardial infarction. Most of the side effects of SAHA are reported in patients with end-stage cancer receiving additional chemotherapeutic agents. In patients taking SAHA chronically and on a regular basis (months or years), deep venous thrombosis, leuko- and thrombocytopenia, bone marrow suppression, and gastrointestinal side effects have been reported.[18] Whereas we do not envision chronic administration, these observations nevertheless highlight the need for careful surveillance for safety.

Effects of HDAC Inhibition on Autophagic Flux and the Consequent Cardioprotective Effects

The adaptive or maladaptive effects of autophagy on cardiac pathology are tightly linked to both the extent of autophagy and the type of stress eliciting the response. Interestingly, there is no consensus regarding whether autophagic flux is increased or impaired during cardiomyocyte reperfusion.[26] Matsui et al[34] demonstrated a clear decrease in infarct size in a mouse model of *BECN1* haploinsufficiency. However, recent studies from Ma et al[35] challenge the assumption that *BECN1* haploinsufficiency merely prevents autophagy initiation, suggesting that it may also act to increase autophagic processing. Ma et al[35] demonstrated that the upregulation of Beclin observed after reperfusion was coupled with a decline in LAMP2 which resulted in diminished autophagic processing. This decrease was rescued by an increase in LAMP2 or a decrease in Beclin1. Our findings support the latter model. Indeed, our findings are in agreement with a number of studies that suggest that an increase in autophagy during I/R is protective.[35–37] Our data show that SAHA treatment increases autophagy specifically in the border zone of I/R-stressed hearts. This increase in autophagy correlates with protection against I/R cell death in vivo and is required for protection by SAHA against cell death in sI/R in vitro.

It is interesting that HDAC inhibition increases autophagic flux primarily in the border zone, where active cell death is taking place. One possible explanation is that cardiomyocytes in the ischemic/infarct zone are lethally injured beyond rescue, whereas uninjured cardiomyocytes in the remote zone lack cues driving autophagosome formation. The sublethally stressed cardiomyocytes in the border zone, however, remain viable and subject to either intracellular or extracellular cues that modulate autophagic flux, a response enhanced by HDAC inhibition.

The ability of SAHA to induce autophagy is consistent with findings in cancer cells treated with SAHA, although the end result of autophagic stimulation in cardiomyocyte I/R appears to be cytoprotective and not cytotoxic as in cancer cells.[38,39] Mechanistic studies in cancer reveal that SAHA elicits the inhibition of mammalian target of rapamycin and the subsequent induction of autophagic flux.[40] Whether this mechanism pertains to cardiomyocytes is currently under investigation.

In contrast to the observations reported here that SAHA induces autophagy on short-term exposure, we have reported previously that chronic HDAC inhibition suppresses autophagy.[30] Whereas, at first glance, these findings appear to be contradictory, closer examination is instructive. First, chronic HDAC inhibition in a pressure overload model in vivo, or in NRVMs in culture, resulted in the reduction of autophagic flux.[30] Here, we exposed mice or rabbits to SAHA transiently. Second, cultured NRVMs in this report were studied in the presence of serum and with only brief serum-free exposure during ischemia. Indeed, we have collected experimental evidence that differences in drug exposure and experimental model are relevant. Nevertheless, both studies point to an intriguing ability of HDAC inhibition to suppress excess autophagic flux or restore impaired autophagic flux to a zone that is beneficial.[2,41]

Other Mechanisms Underlying SAHA Cardioprotection

HDAC inhibition has broad effects on gene expression, and direct effects on protein activity, as well, through the promotion of protein hyperacetylation. Additionally, as yet unidentified off-target effects may exist.[11] It has been reported that SAHA has anti-inflammatory properties.[42,43] However, it is doubtful this accounts for the majority of the cardioprotective effects of SAHA, because solely targeting inflammation during reperfusion injury does not substantially limit infarct size.[44] Further, evaluation here of a selected subset of anti-inflammatory mediators did not reveal significant SAHA-dependent changes (data not shown). Also, SAHA has been suggested to promote the proliferation and homing of stem cells.[33,45] However, given the short duration of our reperfusion injury studies, it seems unlikely that the activation of stem cells plays an important role in SAHA-dependent cardioprotection. Nevertheless, recent studies suggesting that enhanced stem cell activity is critical during the remodeling stage of myocardial infarction open the possibility of benefit from a longer treatment regimen.[33] Our data point to increases in autophagic flux as the primary mechanism of SAHA's cardioprotective effects. Indeed, inhibition of autophagy by specific depletion of ATG7 or ATG5 blocked the ability of SAHA to rescue cells during sI/R. Further work is required to define specific mechanisms, including HDAC protein targets that modulate autophagic flux in cardiomyocyte I/R.

Conclusions and Perspective

Preservation of systolic function post–myocardial infarction correlates with improved clinical outcomes.[46] Here, we demonstrate that an FDA-approved HDAC inhibitor, SAHA, reduces myocardial infarct size in a large-animal model. Reactivation of I/R-triggered downregulated autophagy is a major underlying mechanism. Currently, molecular mechanisms underlying SAHA's cardioprotective effects, and HDAC-dependent control of cardiomyocyte autophagy, remain unknown. However, we

submit that this therapeutic strategy holds promise in addressing the global scourge of ischemic cardiovascular disease.

Acknowledgments

We thank members of the Hill laboratory for helpful discussions and critique. We also thank Colby Ayers for critical advice regarding statistical analyses.

Sources of Funding

This work was supported by grants from the National Institutes of Health (HL-080144, HL-0980842, HL-100401), Cancer Prevention and Research Institute of Texas (RP110486P3), the American Heart Association DeHaan Foundation (0970518 N), and the Fondation Leducq (11CVD04).

Disclosures

None.

References

1. Go AS, Mozaffarian D, Roger VL, Benjamin EJ, Berry JD, Borden WB, Bravata DM, Dai S, Ford ES, Fox CS, Franco S, Fullerton HJ, Gillespie C, Hailpern SM, Heit JA, Howard VJ, Huffman MD, Kissela BM, Kittner SJ, Lackland DT, Lichtman JH, Lisabeth LD, Magid D, Marcus GM, Marelli A, Matchar DB, McGuire DK, Mohler ER, Moy CS, Mussolino ME, Nichol G, Paynter NP, Schreiner PJ, Sorlie PD, Stein J, Turan TN, Virani SS, Wong ND, Woo D, Turner MB; American Heart Association Statistics Committee and Stroke Statistics Subcommittee. Heart disease and stroke statistics–2013 update: a report from the American Heart Association. *Circulation*. 2013;127:e6–e245.
2. Heidenreich PA, Trogdon JG, Khavjou OA, Butler J, Dracup K, Ezekowitz MD, Finkelstein EA, Hong Y, Johnston SC, Khera A, Lloyd-Jones DM, Nelson SA, Nichol G, Orenstein D, Wilson PW, Woo YJ; American Heart Association Advocacy Coordinating Committee; Stroke Council; Council on Cardiovascular Radiology and Intervention; Council on Clinical Cardiology; Council on Epidemiology and Prevention; Council on Arteriosclerosis; Thrombosis and Vascular Biology; Council on Cardiopulmonary; Critical Care; Perioperative and Resuscitation; Council on Cardiovascular Nursing; Council on the Kidney in Cardiovascular Disease; Council on Cardiovascular Surgery and Anesthesia, and Interdisciplinary Council on Quality of Care and Outcomes Research. Forecasting the future of cardiovascular disease in the United States: a policy statement from the American Heart Association. *Circulation*. 2011;123:933–944.
3. Fraccarollo D, Galuppo P, Bauersachs J. Novel therapeutic approaches to post-infarction remodelling. *Cardiovasc Res*. 2012;94:293–303.
4. Dorn GW 2nd. Novel pharmacotherapies to abrogate postinfarction ventricular remodeling. *Nat Rev Cardiol*. 2009;6:283–291.
5. Pfeffer MA, McMurray JJ, Velazquez EJ, Rouleau JL, Køber L, Maggioni AP, Solomon SD, Swedberg K, Van de Werf F, White H, Leimberger JD, Henis M, Edwards S, Zelenkofske S, Sellers MA, Califf RM; Valsartan in Acute Myocardial Infarction Trial Investigators. Valsartan, captopril, or both in myocardial infarction complicated by heart failure, left ventricular dysfunction, or both. *N Engl J Med*. 2003;349:1893–1906.
6. Turer AT, Hill JA. Pathogenesis of myocardial ischemia-reperfusion injury and rationale for therapy. *Am J Cardiol*. 2010;106:360–368.
7. Yellon DM, Hausenloy DJ. Myocardial reperfusion injury. *N Engl J Med*. 2007;357:1121–1135.
8. Schwartz Longacre L, Kloner RA, Arai AE, Baines CP, Bolli R, Braunwald E, Downey J, Gibbons RJ, Gottlieb RA, Heusch G, Jennings RB, Lefer DJ, Mentzer RM, Murphy E, Ovize M, Ping P, Przyklenk K, Sack MN, Vander Heide RS, Vinten-Johansen J, Yellon DM; National Heart, Lung, and Blood Institute, National Institutes of Health. New horizons in cardioprotection: recommendations from the 2010 National Heart, Lung, and Blood Institute Workshop. *Circulation*. 2011;124:1172–1179.
9. Yang XJ, Seto E. Lysine acetylation: codified crosstalk with other post-translational modifications. *Mol Cell*. 2008;31:449–461.
10. Gregoretti IV, Lee YM, Goodson HV. Molecular evolution of the histone deacetylase family: functional implications of phylogenetic analysis. *J Mol Biol*. 2004;338:17–31.
11. McKinsey TA. Therapeutic potential for HDAC inhibitors in the heart. *Annu Rev Pharmacol Toxicol*. 2012;52:303–319.
12. Berry JM, Cao DJ, Rothermel BA, Hill JA. Histone deacetylase inhibition in the treatment of heart disease. *Expert Opin Drug Saf*. 2008;7:53–67.
13. Antos CL, McKinsey TA, Dreitz M, Hollingsworth LM, Zhang CL, Schreiber K, Rindt H, Gorczynski RJ, Olson EN. Dose-dependent blockade to cardiomyocyte hypertrophy by histone deacetylase inhibitors. *J Biol Chem*. 2003;278:28930–28937.
14. Kong Y, Tannous P, Lu G, Berenji K, Rothermel BA, Olson EN, Hill JA. Suppression of class I and II histone deacetylases blunts pressure-overload cardiac hypertrophy. *Circulation*. 2006;113:2579–2588.
15. Zhao TC, Cheng G, Zhang LX, Tseng YT, Padbury JF. Inhibition of histone deacetylases triggers pharmacologic preconditioning effects against myocardial ischemic injury. *Cardiovasc Res*. 2007;76:473–481.
16. Granger A, Abdullah I, Huebner F, Stout A, Wang T, Huebner T, Epstein JA, Gruber PJ. Histone deacetylase inhibition reduces myocardial ischemia-reperfusion injury in mice. *FASEB J*. 2008;22:3549–3560.
17. Seok J, Warren HS, Cuenca AG, Mindrinos MN, Baker HV, Xu W, Richards DR, McDonald-Smith GP, Gao H, Hennessy L, Finnerty CC, López CM, Honari S, Moore EE, Minei JP, Cuschieri J, Bankey PE, Johnson JL, Sperry J, Nathens AB, Billiar TR, West MA, Jeschke MG, Klein MB, Gamelli RL, Gibran NS, Brownstein BH, Miller-Graziano C, Calvano SE, Mason PH, Cobb JP, Rahme LG, Lowry SF, Maier RV, Moldawer LL, Herndon DN, Davis RW, Xiao W, Tompkins RG; Inflammation and Host Response to Injury, Large Scale Collaborative Research Program. Genomic responses in mouse models poorly mimic human inflammatory diseases. *Proc Natl Acad Sci U S A*. 2013;110:3507–3512.
18. Merck Sharp & Dohme Corp. asoMC, Inc. Physician's prescribing information for zolinza® (vorinostat). www.Zolinza.Com/vorinostat/zolinza/consumer/prescribing-zolinza/index/jsp. Accessed October 18, 2012.
19. Wise LD, Turner KJ, Kerr JS. Assessment of developmental toxicity of vorinostat, a histone deacetylase inhibitor, in Sprague-Dawley rats and Dutch Belted rabbits. *Birth Defects Res B Dev Reprod Toxicol*. 2007;80:57–68.
20. Kilgore M, Miller CA, Fass DM, Hennig KM, Haggarty SJ, Sweatt JD, Rumbaugh G. Inhibitors of class 1 histone deacetylases reverse contextual memory deficits in a mouse model of Alzheimer's disease. *Neuropsychopharmacology*. 2010;35:870–880.
21. Chen MY, Liao WS, Lu Z, Bornmann WG, Hennessey V, Washington MN, Rosner GL, Yu Y, Ahmed AA, Bast RC Jr. Decitabine and suberoylanilide hydroxamic acid (SAHA) inhibit growth of ovarian cancer cell lines and xenografts while inducing expression of imprinted tumor suppressor genes, apoptosis, G2/M arrest, and autophagy. *Cancer*. 2011;117:4424–4438.
22. More SS, Itsara M, Yang X, Geier EG, Tadano MK, Seo Y, Vanbrocklin HF, Weiss WA, Mueller S, Haas-Kogan DA, Dubois SG, Matthay KK, Giacomini KM. Vorinostat increases expression of functional norepinephrine transporter in neuroblastoma *in vitro* and *in vivo* model systems. *Clin Cancer Res*. 2011;17:2339–2349.
23. Podesser B, Wollenek G, Seitelberger R, Siegel H, Wolner E, Firbas W, Tschabitscher M. Epicardial branches of the coronary arteries and their distribution in the rabbit heart: the rabbit heart as a model of regional ischemia. *Anat Rec*. 1997;247:521–527.
24. Kelly WK, Richon VM, O'Connor O, Curley T, MacGregor-Curtelli B, Tong W, Klang M, Schwartz L, Richardson S, Rosa E, Drobnjak M, Cordon-Cordo C, Chiao JH, Rifkind R, Marks PA, Scher H. Phase I clinical trial of histone deacetylase inhibitor: suberoylanilide hydroxamic acid administered intravenously. *Clin Cancer Res*. 2003;9(10 pt 1):3578–3588.
25. Rubinsztein DC, Codogno P, Levine B. Autophagy modulation as a potential therapeutic target for diverse diseases. *Nat Rev Drug Discov*. 2012;11:709–730.
26. Przyklenk K, Dong Y, Undyala VV, Whittaker P. Autophagy as a therapeutic target for ischaemia /reperfusion injury? Concepts, controversies, and challenges. *Cardiovasc Res*. 2012;94:197–205.
27. Lopez G, Torres K, Lev D. Autophagy blockade enhances HDAC inhibitors' pro-apoptotic effects: potential implications for the treatment of a therapeutic-resistant malignancy. *Autophagy*. 2011;7:440–441.
28. Shahzad T, Kasseckert SA, Iraqi W, Johnson V, Schulz R, Schlüter KD, Dörr O, Parahuleva M, Hamm C, Ladilov Y, Abdallah Y. Mechanisms involved in postconditioning protection of cardiomyocytes against acute reperfusion injury. *J Mol Cell Cardiol*. 2013;58:209–216.
29. Kang PM, Haunstetter A, Aoki H, Usheva A, Izumo S. Morphological and molecular characterization of adult cardiomyocyte apoptosis during hypoxia and reoxygenation. *Circ Res*. 2000;87:118–125.
30. Cao DJ, Wang ZV, Battiprolu PK, Jiang N, Morales CR, Kong Y, Rothermel BA, Gillette TG, Hill JA. Histone deacetylase (HDAC) inhibitors attenuate cardiac hypertrophy by suppressing autophagy. *Proc Natl Acad Sci U S A*. 2011;108:4123–4128.

31. Xie M, Hill JA. HDAC-dependent ventricular remodeling. *Trends Cardiovasc Med*. 2013;23:229–235.
32. Lee TM, Lin MS, Chang NC. Inhibition of histone deacetylase on ventricular remodeling in infarcted rats. *Am J Physiol Heart Circ Physiol*. 2007;293:H968–H977.
33. Zhang L, Chen B, Zhao Y, Dubielecka PM, Wei L, Qin GJ, Chin YE, Wang Y, Zhao TC. Inhibition of histone deacetylase-induced myocardial repair is mediated by c-kit in infarcted hearts. *J Biol Chem*. 2012;287:39338–39348.
34. Matsui Y, Takagi H, Qu X, Abdellatif M, Sakoda H, Asano T, Levine B, Sadoshima J. Distinct roles of autophagy in the heart during ischemia and reperfusion: roles of AMP-activated protein kinase and Beclin 1 in mediating autophagy. *Circ Res*. 2007;100:914–922.
35. Ma X, Liu H, Foyil SR, Godar RJ, Weinheimer CJ, Hill JA, Diwan A. Impaired autophagosome clearance contributes to cardiomyocyte death in ischemia/reperfusion injury. *Circulation*. 2012;125:3170–3181.
36. Buss SJ, Muenz S, Riffel JH, Malekar P, Hagenmueller M, Weiss CS, Bea F, Bekeredjian R, Schinke-Braun M, Izumo S, Katus HA, Hardt SE. Beneficial effects of Mammalian target of rapamycin inhibition on left ventricular remodeling after myocardial infarction. *J Am Coll Cardiol*. 2009;54:2435–2446.
37. Sala-Mercado JA, Wider J, Undyala VV, Jahania S, Yoo W, Mentzer RM Jr, Gottlieb RA, Przyklenk K. Profound cardioprotection with chloramphenicol succinate in the swine model of myocardial ischemia-reperfusion injury. *Circulation*. 2010;122(11 suppl):S179–S184.
38. Li J, Liu R, Lei Y, Wang K, Lau QC, Xie N, Zhou S, Nie C, Chen L, Wei Y, Huang C. Proteomic analysis revealed association of aberrant ROS signaling with suberoylanilide hydroxamic acid-induced autophagy in Jurkat T-leukemia cells. *Autophagy*. 2010;6:711–724.
39. Thomas S, Thurn KT, Biçaku E, Marchion DC, Münster PN. Addition of a histone deacetylase inhibitor redirects tamoxifen-treated breast cancer cells into apoptosis, which is opposed by the induction of autophagy. *Breast Cancer Res Treat*. 2011;130:437–447.
40. Bánréti A, Sass M, Graba Y. The emerging role of acetylation in the regulation of autophagy. *Autophagy*. 2013;9:819–829.
41. Masiero E, Agatea L, Mammucari C, Blaauw B, Loro E, Komatsu M, Metzger D, Reggiani C, Schiaffino S, Sandri M. Autophagy is required to maintain muscle mass. *Cell Metab*. 2009;10:507–515.
42. Halili MA, Andrews MR, Labzin LI, Schroder K, Matthias G, Cao C, Lovelace E, Reid RC, Le GT, Hume DA, Irvine KM, Matthias P, Fairlie DP, Sweet MJ. Differential effects of selective HDAC inhibitors on macrophage inflammatory responses to the Toll-like receptor 4 agonist LPS. *J Leukoc Biol*. 2010;87:1103–1114.
43. Lin HS, Hu CY, Chan HY, Liew YY, Huang HP, Lepescheux L, Bastianelli E, Baron R, Rawadi G, Clément-Lacroix P. Anti-rheumatic activities of histone deacetylase (HDAC) inhibitors *in vivo* in collagen-induced arthritis in rodents. *Br J Pharmacol*. 2007;150:862–872.
44. Timmers L, Pasterkamp G, de Hoog VC, Arslan F, Appelman Y, de Kleijn DP. The innate immune response in reperfused myocardium. *Cardiovasc Res*. 2012;94:276–283.
45. Burba I, Colombo GI, Staszewsky LI, De Simone M, Devanna P, Nanni S, Avitabile D, Molla F, Cosentino S, Russo I, De Angelis N, Soldo A, Biondi A, Gambini E, Gaetano C, Farsetti A, Pompilio G, Latini R, Capogrossi MC, Pesce M. Histone deacetylase inhibition enhances self renewal and cardioprotection by human cord blood-derived CD34 cells. *PLoS One*. 2011;6:e22158.
46. Otterstad JE, Ford I. The effect of carvedilol in patients with impaired left ventricular systolic function following an acute myocardial infarction. How do the treatment effects on total mortality and recurrent myocardial infarction in CAPRICORN compare with previous beta-blocker trials? *Eur J Heart Fail*. 2002;4:501–506.

CLINICAL PERSPECTIVE

Coronary artery disease is the leading cause of heart failure that stems from reduced contractile performance of the heart. In this setting, reduced blood flow to the heart (ischemia) is typically followed by reperfusion, when the infarct-related artery recannulates, either spontaneously or in response to therapeutic intervention. This event, which restores oxygen and nutrients to the injured tissue, triggers a complex cascade of events and a second wave of injury. Indeed, cell death occurring during reperfusion is a major contributor to infarct size, approaching 50% of total injury burden. Yet, no standard therapies are available targeting reperfusion injury. We report that suberoylanilide hydroxamic acid, a histone deacetylase inhibitor approved by the US Food and Drug Administration for cancer treatment, reduces myocardial infarct size in a large-animal model, specifically by blunting reperfusion injury. Reactivation of ischemia/reperfusion–triggered downregulation of the intracellular protein recycling pathway, autophagy, is a major underlying mechanism. We submit that this therapeutic strategy holds promise in addressing the global scourge of ischemic cardiovascular disease.

Online Data Supplement

.....

HDAC inhibition blunts ischemia/reperfusion injury by inducing cardiomyocyte autophagy

Min Xie, MD, PhD[a], Yongli Kong, MD[a], Wei Tan, MD[a], Herman May, BS[a], Pavan K. Battiprolu, PhD[a], Zully Pedrozo, PhD[a], Zhao Wang, PhD[a], Cyndi Morales, BS[a], Xiang Luo, MD[a], Geoffrey Cho, MD[a], Nan Jiang, MS[a], Michael E. Jessen, MD[b], John J. Warner, MD[a], Sergio Lavandero[a,c], PhD, Thomas G. Gillette, PhD[a], Aslan T. Turer, MD[a], and Joseph A. Hill, MD, PhD[a,d]

Departments of [a]Internal Medicine (Cardiology), [b]Cardiovascular and Thoracic Surgery, [c]Centro Estudios Moleculares de la Célula, Facultad de Ciencias Químicas y Farmacéuticas & Facultad de Medicina, Universidad de Chile, Santiago, Chile, and [d]Department of Molecular Biology, University of Texas Southwestern Medical Center, Dallas, Texas

Address correspondence to:
Joseph A. Hill, MD, PhD
Division of Cardiology
University of Texas Southwestern Medical Center
NB11.200
6000 Harry Hines Boulevard
Dallas, TX 75390-8573, USA
joseph.hill@utsouthwestern.edu

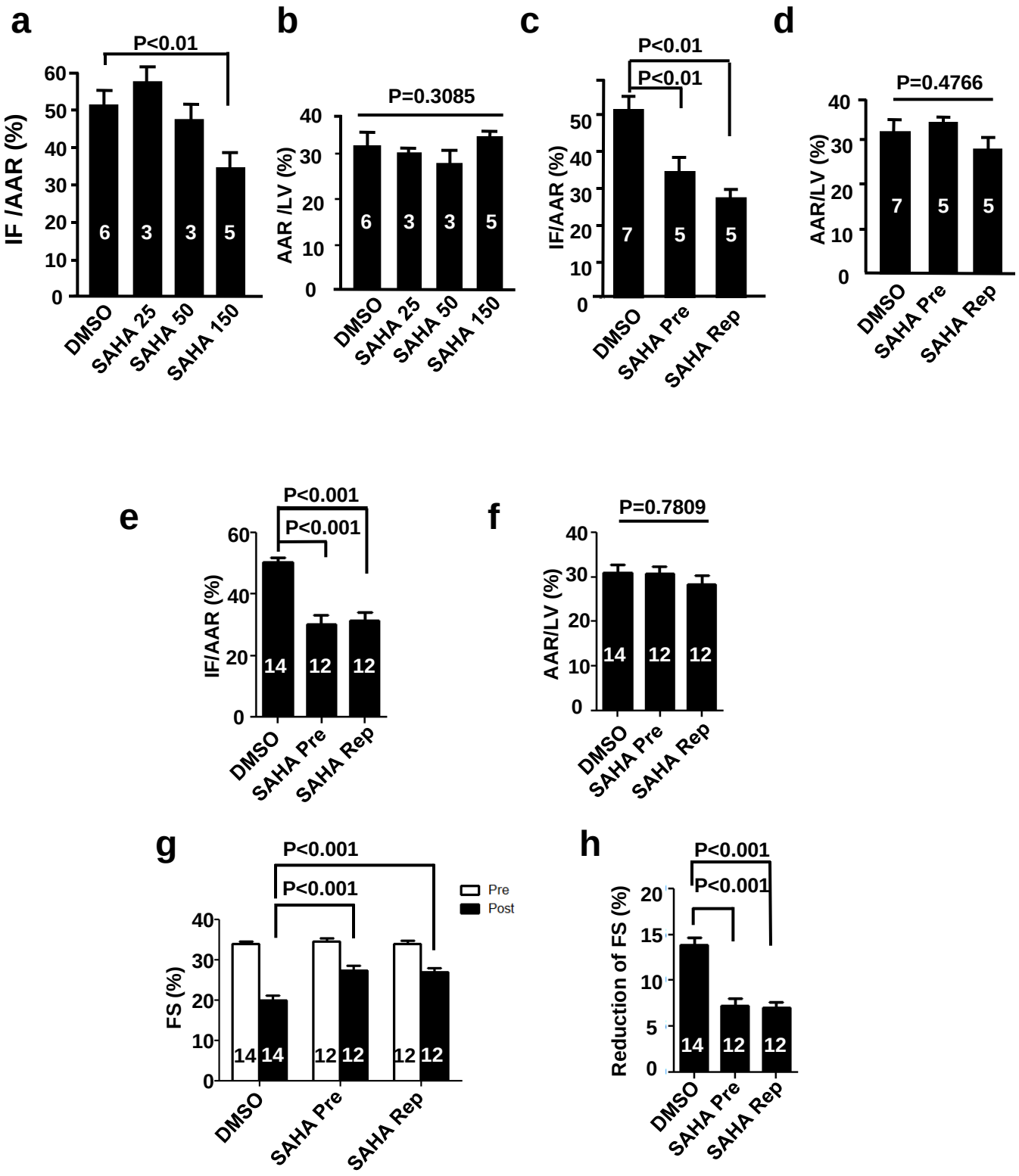

Supplemental Figure 1. SAHA reduces infarct size in rabbit I/R model

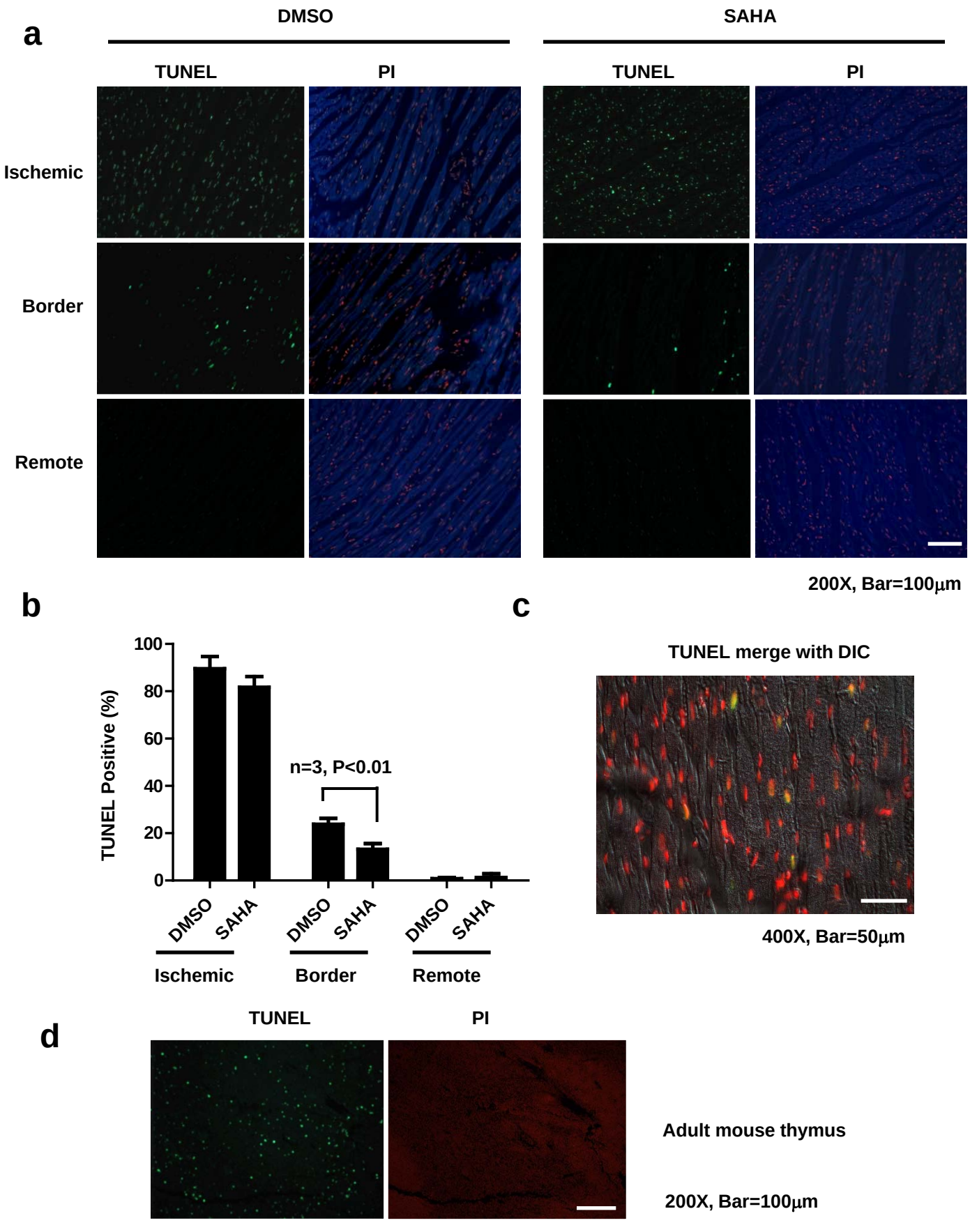

Supplemental Figure 2. SAHA decreases apoptosis by TUNEL.

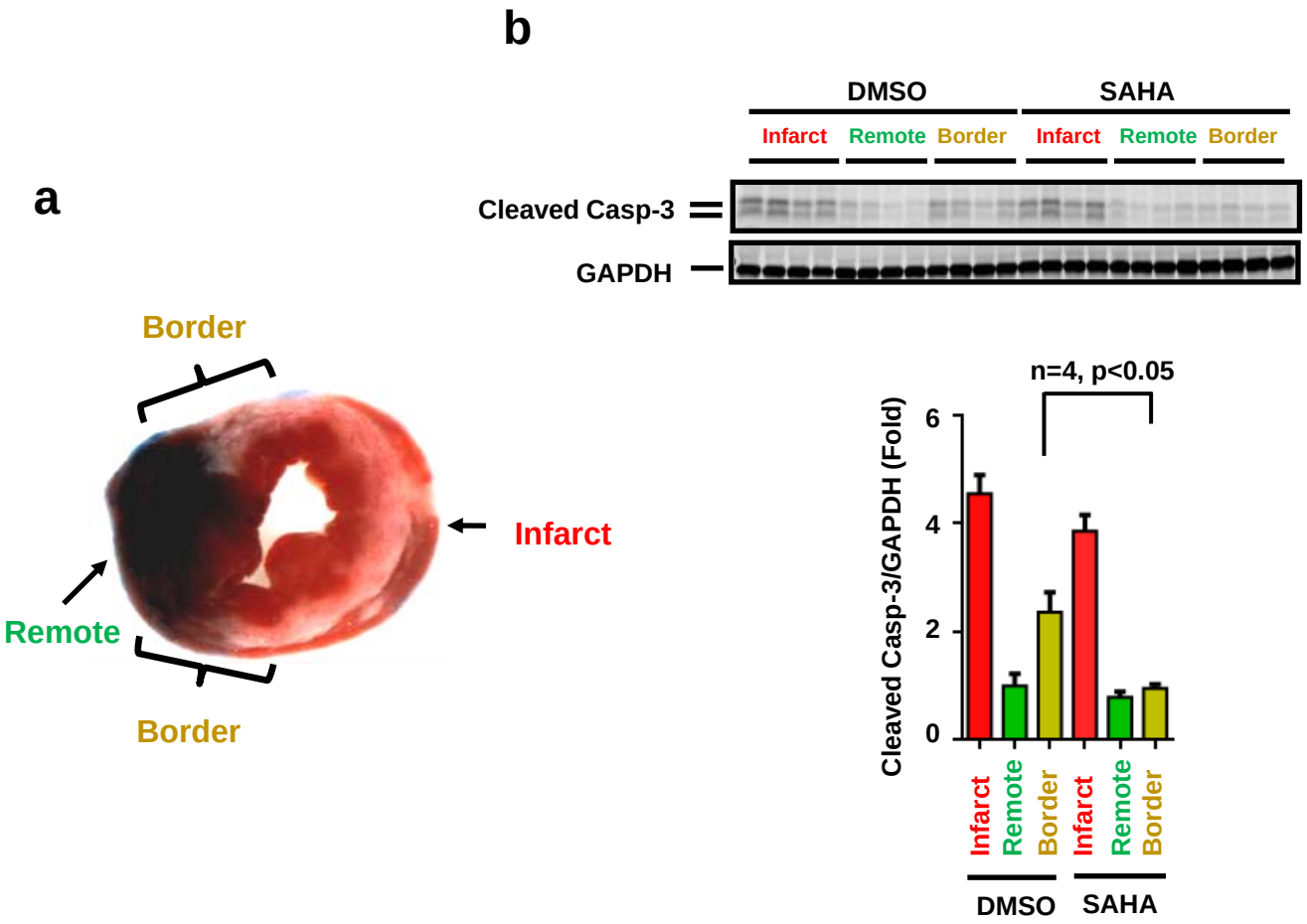

Supplemental Figure 3. SAHA decreased apoptosis in the infarct border zone as measured by cleaved caspase-3.

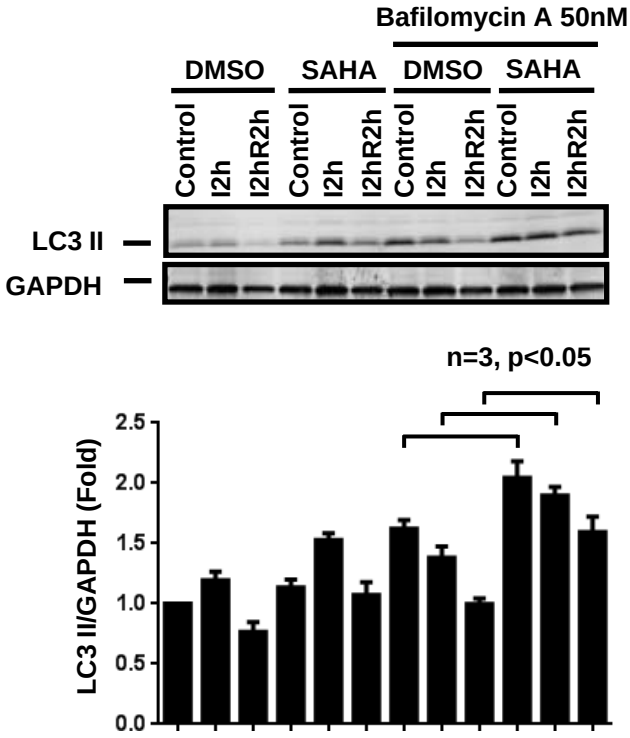

Supplemental Figure 4. SAHA induces autophagic flux in adult rat ventricular myocytes subjected to simulated IR

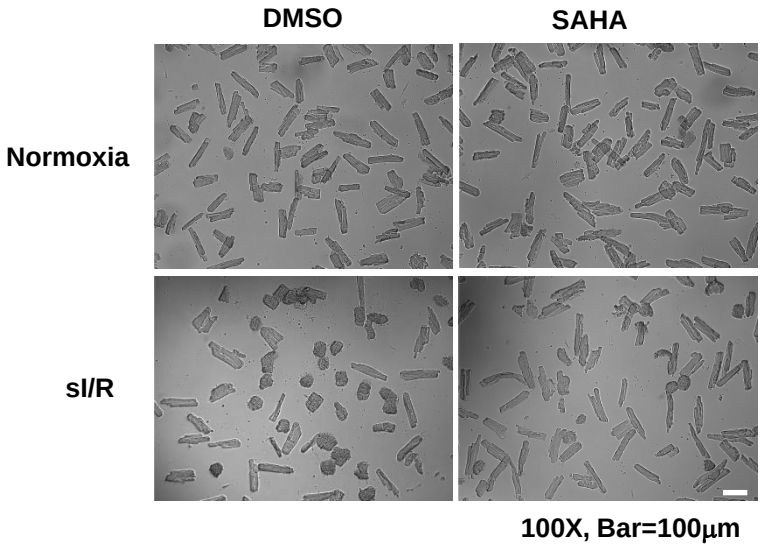

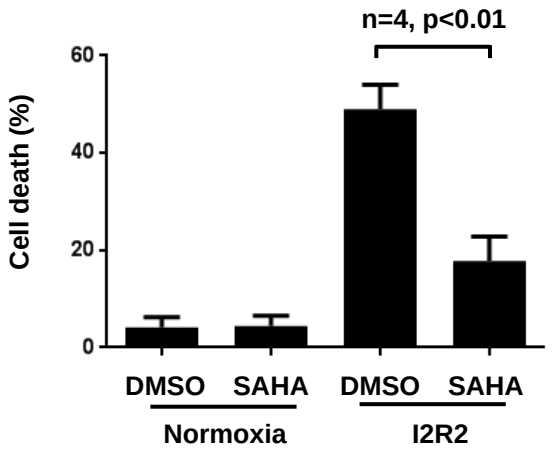

Supplemental Figure 5. SAHA protects ARVMs from cell death after simulated IR

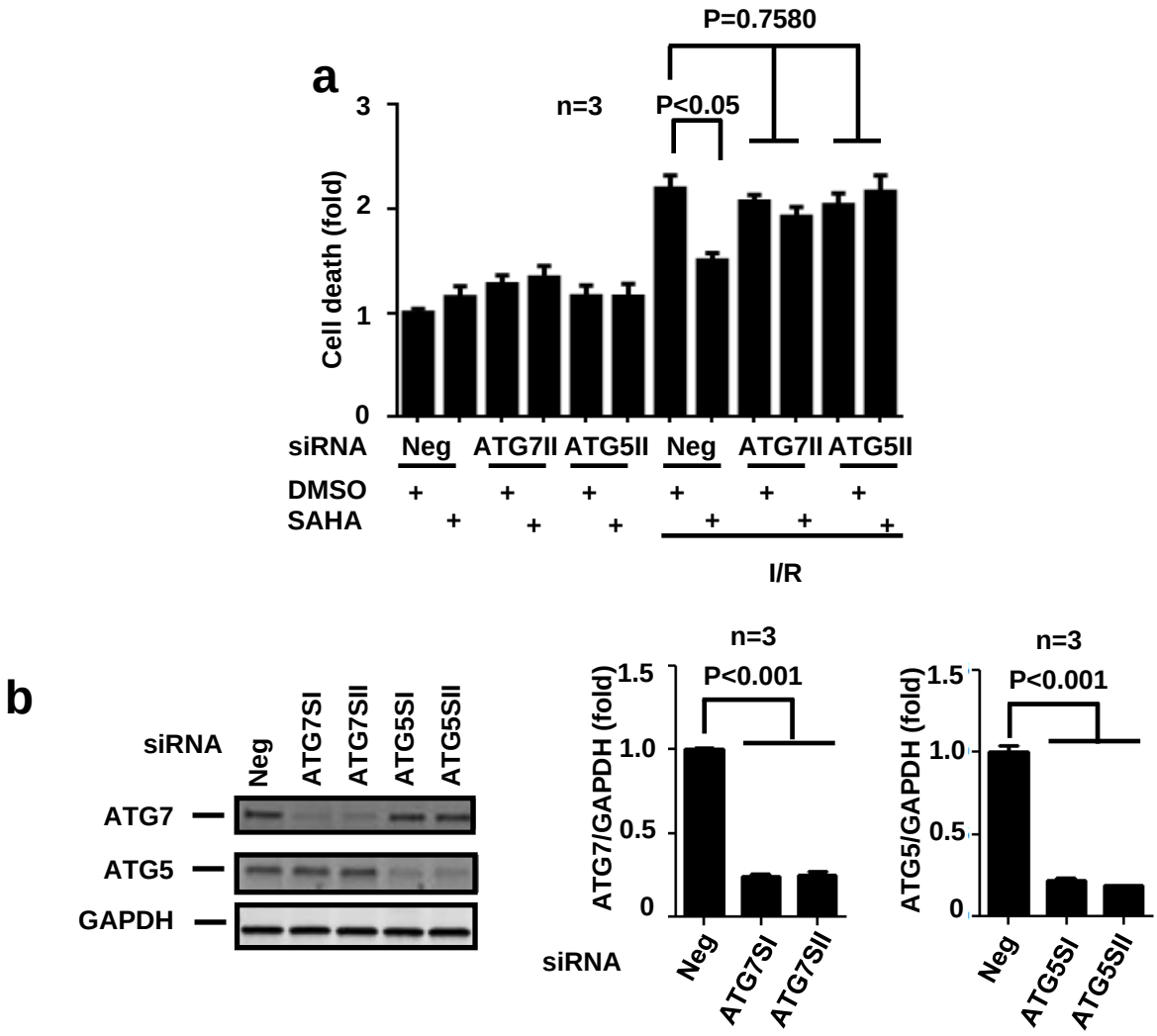

Supplemental Figure 6. SAHA's cardioprotective effects are dependent on autophagic flux as tested using a second, sequence-independent set of ATG7 and ATG5 siRNAs.

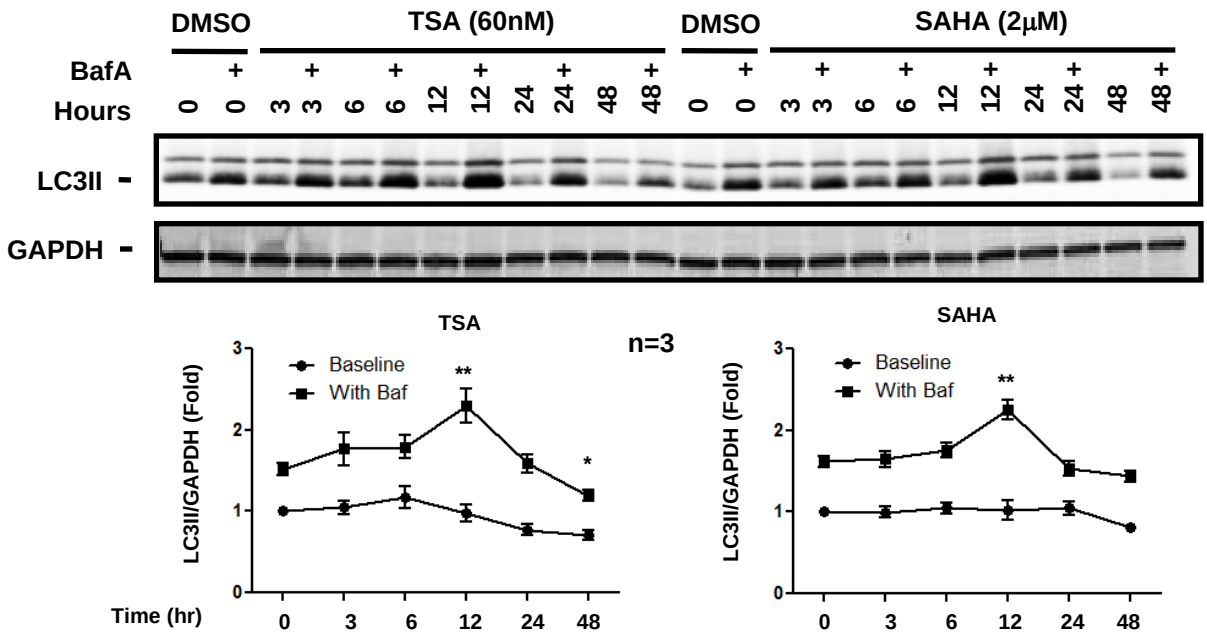

Supplemental Figure 7. TSA and SAHA induce autophagic flux at early time points, and prolonged TSA treatment reduces autophagic flux in serum-free conditions.

	Study Type	n	Shapiro-Wilk normality	Test used	Significance
Figure 1bcd	Mouse	11	Passed	Parametric Unpaired t test	p<0.05 DMSO vs TSA
Figure 1e	Mouse	10	Passed	Parametric Repeated measure ANOVA	p<0.05 DMSO vs TSA at all four time points
Figure 1ghi	Mouse	6-7	SAHA 30 passed, DMSO, SAHA50 n too small	Non-parametric Anova Kruskal-Wallis test	IF/AAR, FS p<0.05 DMSO vs SAHA50
Figure 3bcdfg	Rabbit	7	All group passed	Parametric ANOVA with post Tukey's multiple comparisons test	IF/AAR, IF/LV and FS p<0.05 DMSO vs SAHA pre and SAHA reper
Figure5a	Molecular	4	n too small	Parametric ANOVA with post Tukey's multiple comparisons test	p<0.05 SAHA border vs DMSO border
Figure5d	Molecular	3-5	n too small	Parametric ANOVA with post Tukey's multiple comparisons test	p<0.05 Autophagosome Autolysosome DMSO vs SAHA reper and SAHA pre
Figure6a	Molecular	3 (triplicate 9)	All group passed	Parametric ANOVA with post Tukey's multiple comparisons test	p<0.05 DMSO vs SAHA
Figure6b	Molecular	3	n too small	Parametric ANOVA with post Tukey's multiple comparisons test	p<0.05 DMSO vs SAHA
Figure6c	Molecular	3	n too little	Parametric ANOVA with post Tukey's multiple comparisons test	p<0.05 DMSO vs SAHA
Figure6d	Molecular	3 (triplicate 9)	All group passed	Parametric ANOVA with post Tukey's multiple comparisons test	p<0.05 DMSO vs SAHA
Figure6e	Molecular	4	n too small	Parametric ANOVA with post Tukey's multiple comparisons test	p<0.05 Control vs ATG7 and ATG5
Figure7a	Molecular	3	n too small	Parametric ANOVA with post Tukey's multiple comparisons test	p<0.05 DMSO vs SAHA
Figure7b	Molecular	3 (triplicate 9)	All group passed	Parametric ANOVA with post Tukey's multiple comparisons test	p<0.05 hypo DMSO neg vs hypo SAHA neg
Supp Figure 1ab	Rabbit	3-6	n too small	Non-Parametric Mann Whitney t test between DMSO and SAHA 150	p<0.05 DMSO vs SAHA150
Supp Figure 1cd	Rabbit	5-7	n too small	Non-Parametric Kruskal-Wallis test with Dunn's multiple comparisons test	p<0.05 DMSO vs SAHA reper and SAHA pre
Supp Figure 1efgh	Rabbit	12-14	All group passed	Parametric ANOVA with post Tukey's multiple comparisons test	p<0.05 DMSO vs SAHA reper and SAHA pre
Supp Figure 2	Molecular	3	n too small	Parametric ANOVA with post Tukey's multiple comparisons test	p<0.05 DMSO border vs SAHA border
Supp Figure 3	Molecular	3	n too small	Parametric ANOVA with post Tukey's multiple comparisons test	p<0.05 DMSO border vs SAHA border
Supp Figure 4	Molecular	3	n too small	Parametric ANOVA with post Tukey's multiple comparisons test	p<0.05 DMSO vs SAHA across neg, I2 and I2R2
Supp Figure 5	Molecular	4 (triplicate 12)	All group passed	Parametric ANOVA with post Tukey's multiple comparisons test	p<0.05 DMSO vs SAHA after I2R2
Supp Figure 6a	Molecular	3 (triplicate 9)	All group passed	Parametric ANOVA with post Tukey's multiple comparisons test	p<0.05 DMSO vs SAHA
Supp Figure 6b	Molecular	3	n too small	Parametric ANOVA with post Tukey's multiple comparisons test	p<0.05 Neg vs ATG7 and ATG5
Supp Figure 7	Molecular	3	n too small	t test between each time point to time 0h	p<0.05 TSA time 12h and 48h vs time 0h,SAHA 12h vs 0h

Supplemental Table 1. Experiment paradigm and statistical methods used

	Study Type	n	Shapiro-Wilk normality	Non-parametric Test used	Significance (exact p value)
Figure 1b	Mouse (TSA infarct size)	11	Passed	Mann Whitney test	IF/AAR, DMSO vs TSA, p=0.0128
Figure 1e	Mouse (TSA FS)	10	Passed	Friedman test, with Dunn's post test of two groups	FS, DMSO vs TSA, Day1 p=0.0394, Day3 p=0.0052, Day7 p=0.0001, Day14 p=0.024
Figure 1g	Mouse (SAHA infarct size)	6-7	SAHA 30 passed, DMSO, SAHA50 n too small	Anova Kruskal-Wallis test, with Dunn's post test of two groups	IF/AAR, DMSO vs SAHA50, p=0.0179
Figure 1i	mouse (SAHA FS)	6-7	SAHA 30 passed, DMSO, SAHA50 n too small	Anova Kruskal-Wallis test, with Dunn's post test of two groups	Post IR FS, DMSO vs SAHA Pre, p=0.0381
Figure 3b	Rabbit (SAHA infarct size)	7	All group passed	Anova Kruskal-Wallis test, with Dunn's post test of two groups	IF/AAR, DMSO vs SAHA Pre, p=0.0015, DMSO vs SAHA Reper, p=0.0423
Figure 3f	Rabbit (SAHA FS)	7	All group passed	Anova Kruskal-Wallis test, with Dunn's post test of two groups	Post IR FS, DMSO vs SAHA Pre, p=0.0083, DMSO vs SAHA Reper, p=0.0025

Supplemental Table 2. Non-parametric statistical analyses of all animal studies

Supplemental Figure Legends

Supplemental Figure 1. SAHA reduces infarct size in rabbit I/R model. a. SAHA pretreatment reduced infarct size normalized to area at risk (IF/AAR) as determined by TTC staining (n=3-6, $p<0.05$). All rabbits were subjected to I/R (30 min/24 hour). **b.** There were no significant differences in AAR among groups. **c.** In a non-randomized cohort, both SAHA pretreatment and reperfusion-only treatment reduced IF/AAR (n=5-7, $p<0.01$). **d.** There were no significant differences in AAR among groups. **e**. Data from both randomized and non-randomized cohorts are combined. SAHA reduced IF/AAR significantly (n=12-14, $p<0.001$). **f.** There were no significant differences in AAR among groups. **g.** Data from both randomized and non-randomized cohorts are combined. SAHA partially preserved systolic function quantified as %FS (n=12-14, $p<0.001$). **h**. Declines in contractile performance after I/R, measured as %FS, were significantly blunted in the SAHA treatment group (n=12-14, $p<0.001$).

Supplemental Figure 2. SAHA decreases apoptosis by TUNEL. a. TUNEL staining of three tissue zones: infarct zone, border zone, and remote zone. Green, TUNEL-positive nuclei, Red, PI staining of nuclei. Rabbits were subjected to I/R (30 min/2 hour). **b.** Quantification of TUNEL-positive nuclei. SAHA treatment significantly reduced TUNEL-positive nuclei in the I/R border zone (n=3, $p<0.01$). **c.** Merged image of DIC and TUNEL staining reveals that TUNEL-positive cells are predominantly within striated myocytes. **d.** Adult mouse thymus was used as a positive control for TUNEL staining.

Supplemental Figure 3. SAHA decreased apoptosis in the infarct border zone as measured by cleaved caspase-3. a. Rabbit myocardium samples were harvested as depicted. Red: infact zone, Green: remote zone, Yellow: border zone. **b. Upper:** Immunoblot analysis of cleaved caspase 3. **Lower:** Quantification of cleaved caspase 3 revealed that levels were significantly lower in the SAHA-treated group (n=4, $p<0.05$).

Supplemental Figure 4. SAHA induces autophagic flux in adult rat ventricular myocytes subjected to simulated IR. Upper: Western blots. **Lower:** mean data. SAHA pretreatment induced autophagic flux in ARVMs at baseline and after simulated ischemia 2hr (I2h). Furthermore, SAHA treatment exclusively at reperfusion induced autophagic flux after simulated ischemia (2hr) plus reperfusion (2hr) [I2R2].

Supplemental Figure 5. . SAHA protects ARVMs from cell death after simulated IR. SAHA treatment (2μM) at reperfusion reduced cell death around 60% after simulated I/R (sI/R; 2hour/2 hour) (n=4, $p<0.05$).

Supplemental Figure 6. . SAHA's cardioprotective effects are dependent on autophagic flux as tested using a second, sequence-independent set of ATG7 and ATG5 siRNAs. a. LDH cell death assays were conducted in the settings of ATG7 or ATG5 knockdown using sequence-independent siRNA constructs (ATG7II and ATG5II). Suppression of either ATG7 or ATG5 abolished SAHA's cardioprotective effects after sI/R (5 hour/1.5 hour) (n=3, $p<0.05$). **b.** RNAi knockdown of ATG7 or ATG5 using ATG7II and ATG5II siRNA. This independent set of siRNAs suppressed ATG7 and ATG5 levels as efficiently as the original set of constructs. **Left:** Western blots. **Right:** mean data.

Supplemental Figure 7. TSA and SAHA induce autophagic flux at early time points, and prolonged TSA treatment reduces autophagic flux in serum-free conditions. Upper: Autophagic flux measurement by LC3 II Western blot in the presence/absence of Bafilomycin A (Bfa) in NRVM treated with TSA. **Lower:** Quantification (n=3). **, $p<0.01$; *, $p<0.05$ compared with DMSO control.

Supplemental Tables

Supplemental Table 1. Experiment paradigm and statistical methods used. Methods employed in each figure are listed. In the animal studies, if the data did not pass criteria for normality, non-parametric analysis was performed. In the molecular studies, parametric analyses were performed throughout. The cell death assay data fulfilled normality. Statistical significance is reported if $p<0.05$.

Supplemental Table 2. Non-parametric statistical analyses of all animal studies. As the animal sample sizes are low, and in an effort to maximize stringency, we also conducted non-parametric analyses in all animal studies. In each case, these analyses confirmed the statistical significance derived from parametric analyses.